

Utah State University

DigitalCommons@USU

All Graduate Theses and Dissertations

Graduate Studies

8-2022

Upstream Methods for Enhancing Engineered Curcumin Biosynthesis

Caleb D. Barton
Utah State University

Follow this and additional works at: <https://digitalcommons.usu.edu/etd>



Part of the [Biological Engineering Commons](#)

Recommended Citation

Barton, Caleb D., "Upstream Methods for Enhancing Engineered Curcumin Biosynthesis" (2022). *All Graduate Theses and Dissertations*. 8588.

<https://digitalcommons.usu.edu/etd/8588>

This Thesis is brought to you for free and open access by the Graduate Studies at DigitalCommons@USU. It has been accepted for inclusion in All Graduate Theses and Dissertations by an authorized administrator of DigitalCommons@USU. For more information, please contact digitalcommons@usu.edu.



UPSTREAM METHODS FOR ENHANCING ENGINEERED CURCUMIN
BIOSYNTHESIS

by

Caleb D. Barton

A thesis submitted in partial fulfillment
of the requirements for the degree

of

MASTER OF SCIENCE

in

Biological Engineering

Approved:

Jixun Zhan, Ph.D.
Major Professor

Ron Sims, Ph.D.
Committee Member

Anhong Zhou, Ph.D.
Committee Member

Justin Jones, Ph.D.
Committee Member

D. Richard Cutler, Ph.D.
Vice Provost of Graduate Studies

UTAH STATE UNIVERSITY
Logan, Utah

2022

Copyright © Caleb D. Barton 2022

All Rights Reserved

ABSTRACT

Upstream Methods for Enhancing Engineered Curcumin Biosynthesis

by

Caleb D. Barton, Master of Science

Utah State University, 2022

Major Professor: Dr. Jixun Zhan
Department: Biological Engineering

Curcumin is an extremely versatile natural compound possessing several therapeutic benefits ranging from anti-cancer potential to anti-Alzheimer's properties. Though it occurs naturally in the roots of *Curcuma longa*, curcumin may be biosynthesized in the heterologous host *Escherichia coli*. However, insufficient amounts of curcumin have been obtained from the heterologous system up to now.

Various upstream methods were employed to enhance the production of curcumin in an engineered *E. coli* platform. First, the enzymatic approach for achieving curcumin biosynthesis was optimized. Plant enzymes were explored in combination with bacterial enzymes to find the most productive enzymatic approach. Specifically, the productivity of bacterial feruloyl-CoA synthase (FCS) was compared with that of the plant 4-coumarate-CoA ligase (4CL), and curcuminoid synthase (CUS) was compared with diketide-CoA synthase (DCS) and curcumin synthase (CURS1). Additionally, the use of transferase co-expression systems was used to study the effect of appending sugar or sulfate moieties to curcumin to enhance the water solubility and thus facilitate its export from the cell, allowing for continuous fermentation and reducing the cytotoxic effects of intracellular curcumin accumulation. Specifically, the use of a glucosyltransferase from *Beauveria bassiana*, a glucuronyltransferase from *Streptomyces chromofuscus*, and a sulfotransferase from *Haliangium ochraceum* and each of their impacts on curcumin production was discussed.

(74 pages)

PUBLIC ABSTRACT

Upstream Methods for Enhancing Engineered Curcumin Biosynthesis

Caleb D. Barton

Curcumin is a bright orange compound with myriad applications for human health and wellness. Curcumin occurs naturally in the plant *Curcuma longa* (commonly known as turmeric) but must be extracted from the roots in an environmentally unfriendly fashion to obtain commercially relevant amounts of the compound. In addition, extraction of curcumin from turmeric spice yields a mixture of various curcuminoids, presenting an issue for isolating it in its pure form and complicating its use in clinical settings.

Heterologous biosynthetic production of curcumin in *Escherichia coli* has been used extensively as a viable alternative to plant extraction but suffers from poor yield. This thesis describes the application of various upstream biological engineering methods for enhancing the production of curcumin in an engineered *E. coli* platform. Among these, the enzyme combination for achieving curcumin biosynthesis is optimized, including the use of bacterial and plant enzymes for improving the overall yield. Since curcumin is mainly produced as an intracellular metabolite with cytotoxic effects on the production host, the use of a handful of transferases that can improve curcumin water solubility is also explored to improve excretion from the cell.

These approaches led to the establishment of an efficient curcumin biosynthetic pathway, the identification of several feruloyl-CoA synthases (FCSs) that may be used in place of 4-coumarate-CoA ligase (4CL), and methods for improving curcumin excretion from the cell together with more bioavailable curcumin derivatives. We also discuss the use of a bacterial long-chain fatty acid-CoA ligase for the efficient production of a curcuminoid known as dicinnamoylmethane.

This thesis is dedicated to my wife, Kami Lay, and to our son Kai.

ACKNOWLEDGMENTS

It goes without saying that Dr. Jixun Zhan has been an immense support throughout the completion of this thesis research. I want to thank Dr. Zhan for his patience and kindness at every point during this process. He has fueled my success and guided me through every step of the project, providing critical feedback and suggestions to keep the research moving along.

I would also like to thank the graduate committee members for their individual contributions to my overall success: Dr. Ron Sims for teaching me fundamental skills about fermentation and biochemical engineering; Dr. Anhong Zhou for teaching me the principles of biosensors and data collection; and Dr. Justin Jones for teaching me everything I know about proteins, their function, structure, and purification. Each committee member has been extremely friendly and encouraging towards me, for which I am grateful.

I also want to thank Jie Ren for teaching me each of the procedures used in the Metabolic Engineering Laboratory. Jie has been an incredible source of knowledge for accomplishing the hands-on research and has been patient with me as he has worked by my side daily. Above all, Jie has been a friend to me, for which I am deeply appreciative.

For supporting my research and being an outstanding mentee, I would like to thank Ceaira Howard. Ceaira has kept all my buffers, plasmids, and strains in stock and has lent an extra hand on countless occasions. Her contributions have been invaluable for helping me be efficient in my research.

Lastly, deep thanks to my supportive wife Kami Lay. Her sacrifice has exceeded my own as she has endured many late-night trips to the lab. Thanks to her extensive laboratory experience as a Biological Engineering undergraduate, Kami has also provided hands-on support with my research whenever possible and has encouraged me to work hard and be patient with myself and others.

Caleb D. Barton

CONTENTS

	Page
Abstract.....	i
Public Abstract.....	iv
Acknowledgments.....	vi
Contents	v
List Of Tables	ix
List Of Figures	x
Chapter I Introduction.....	1
Chapter II Literature Review	4
2.1 Medical Relevance of Curcumin.....	4
2.2 Curcumin Production and Isolation.....	6
2.3 Heterologous Curcumin Biosynthesis in <i>E. coli</i>	8
2.4 Curcumin Hydrophobicity and Cytotoxic Effect on Production Host	11
Chapter III Experimental Methods	13
3.1 Genomic DNA Extraction.....	13
3.2 Identification and Cloning of Putative FCS Genes from Various Hosts	14
3.3 Plasmid Construction, Transformation, and Purification.....	16
3.4 Induction of Expression	17
3.5 Enzyme Purification and Kinetic Assays	18
3.7 Statistical Methods	21
Chapter IV Results	22
4.1 Identification of an Efficient FCS from <i>Bradyrhizobium japonicum</i> USDA 6.....	22
4.2 Kinetic Parameters of 4507FCS v. At4CL1 <i>in vitro</i>	24
4.3 Investigation of StlB for Curcuminoid Production	26
4.4 Optimization of the Curcumin Biosynthesis Enzymatic Approach	27
4.5 Glycosylation of Curcumin <i>In Vivo</i>	30
4.6 Sulfation of Curcumin <i>In Vivo</i>	32
4.7 Effect of Transferase Co-Expression on Curcumin Excretion.....	36

4.8 Effect of Transferase Co-Expression on Total Curcumin Yield	40
Chapter V Conclusions.....	43
Chapter VI Engineering Value and Future Work	46
6.1 Engineering Value.....	46
6.2 Future Work	47
6.2.1 Individual Enzyme Expression Optimization	47
6.2.2 Improving Curcumin Glycoside and Curcumin Sulfate Production	47
6.2.3 Structural Studies and Enzyme Engineering.....	48
6.2.4 Biochemical Process Development and Optimization	48
References.....	50
Appendices.....	59
Appendix A. Supplemental Spectral Data.....	60

LIST OF TABLES

	Page
Table 3.1 Gene locii and GenBank accession numbers for target genes	13
Table 3.2 Culture media used for obtaining gDNAs	14
Table 3.3 Primers and plasmids used in this thesis.....	15
Table 3.4 General PCR Reaction Scheme	16
Table 3.5 Ligation Reaction Scheme	16
Table 4.1 Enzyme kinetics for At4CL1 and 4507FCS.....	26
Table 4.2 Summary of StlB substrate flexibility testing.....	27
Table 4.3 Enzymatic approaches for achieving curcumin biosynthesis.	28
Table 4.4 Mean curcumin yields for each enzymatic approach.....	28
Table 4.5 Curcumin glycoside and sulfate product peak areas.....	38

LIST OF FIGURES

	Page
Figure 1.1: Chemical structure of a variety of curcuminoids	2
Figure 2.1: Summary of the health-promoting properties of curcumin	6
Figure 2.2: Two enzymatic approaches for achieving curcumin biosynthesis.	8
Figure 2.3: Production of various curcuminoids from amino acid precursors	10
Figure 4.1: FCS functional screening	22
Figure 4.2: FCS curcumin yield comparisons.....	23
Figure 4.3: SDS-PAGE analysis of purified At4CL1 and 4507FCS	24
Figure 4.4: Lineweaver-Burke Plots for At4CL1 and 4507FCS.....	25
Figure 4.5: Curcumin yield comparisons for various enzymatic approaches.....	29
Figure 4.6: Formation of curcumin and curcumin glucoside.....	31
Figure 4.7: Formation of curcumin and curcumin glucuronide	32
Figure 4.8: Biotransformation of curcumin into curcumin sulfate	34
Figure 4.9: Curcumin sulfate production over time.....	35
Figure 4.10: Curcumin di-sulfate production.....	36
Figure 4.11: Effect of transferase co-expression on curcumin excretion	37
Figure 4.12: Visual representation of curcumin excretion based on transferase co-expression ...	39
Figure 4.13: Total curcumin yield for each transferase treatment group.....	40
Figure 4.14: Proposed glycosylation pathways	41
Figure 4.15: Glycosylation of ferulic acid	42
Figure A.1: Confirmation of curcumin formation by StlB + CUS	60
Figure A.2: Confirmation of bisdemethoxycurcumin formation by StlB + CUS.....	61

Figure A.3: No dicaffeoylmethane formation by StlB + CUS.....	62
Figure A.4: Confirmation of dicinnamoylmethane formation by StlB +CUS.....	63

CHAPTER I

Introduction

The natural world contains an amazing repository of natural products that forms the basis of many supplements, pharmaceuticals, and therapeutics in use today. Drug discovery and development has often relied on biomolecules obtained from nature, beginning with the discovery of penicillin in 1929 and continuing to the present day. Among these, the polyketide family is of special interest. Polyketides are a group of acetate-derived, structurally diverse natural compounds exhibiting a broad spectrum of bioactivities.¹ These multi-faceted compounds can be derived from plants, fungus, and bacteria. Polyketides are synthesized by polyketide synthases (PKSs), which are generally multi-domain enzymes that can be categorized into three types. Type I PKSs are large, modular enzymes that pass molecules through a series of catalytic domains, while Type II PKSs are smaller and form multienzyme complexes capable of producing aromatic polyketides. Type III PKSs form homodimers, and act in an iterative fashion to prime, extend, and cyclize their targets.²

One member of the polyketide family is a health-promoting, aromatic plant polyketide known as curcumin that is formed by the action of Type III plant PKSs.³ This bright orange compound is commonly harvested from the rhizome of *Curcuma longa* (turmeric spice) together with other aromatic polyketides that share a similar core structure, known as curcuminoids. Curcuminoids (most especially curcumin) have been reported to possess myriad health benefits, most importantly anticancer properties, making them interesting targets for pharmaceutical research (**Fig. 1.1**).

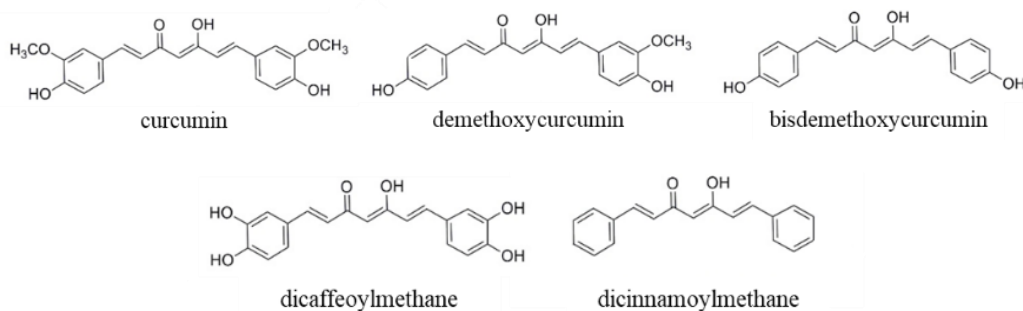


Figure 1.1: Chemical structure of a variety of curcuminoids

Ongoing academic and clinical studies on curcumin and other curcuminoids have created an increased need for pure curcuminoid products and improved methods for their production and isolation. Heterologous production of curcuminoids in *Escherichia coli* has garnered special interest in the last several years but has not been able to produce commercially relevant titers of the compounds for competing with the agricultural methods commonly used for their production. Heterologous biosynthesis has several benefits over agricultural methods, including reduced time scale, land use, and organic solvent consumption.

This thesis explores a variety of upstream biological engineering approaches to improving heterologous curcuminoid biosynthesis in *E. coli* with special focus on curcumin. Herein, we utilize several enzymatic approaches for enhancing engineered curcuminoid production. Among these, we discuss the use of several enzymatic approaches employing combinations of both plant and bacterial proteins to achieve curcumin biosynthesis. Specifically, we compare the use of feruloyl-CoA synthase (FCS) in place of the 4-coumarate-CoA ligase (4CL) commonly used for catalyzing the formation of feruloyl-CoA from ferulic acid. We also demonstrate the importance of diketide-CoA synthase (DCS) as an important enzymatic factor for enhancing curcumin production. We also make quantitative comparisons between the productivity of curcuminoid synthase (CUS) and curcumin synthase (CURS1). Additionally, we explore methods for excreting

curcumin from *E. coli*, which is produced primarily as an intracellular metabolite, exerting a cytotoxic effect on the production host. These methods include glucosylation, glucuronidation, and sulfation to assist in the development of continuous fermentation production processes.

CHAPTER II

Literature Review

2.1 Medical Relevance of Curcumin

Curcumin has long been known for its amazing therapeutic properties.⁴ Most notably recognized for its anti-cancer,⁵ anti-inflammatory,⁶ antidiabetic,⁷ and anti-Alzheimer's properties,⁸ curcumin is an important and multi-faceted drug target. Ongoing research continuously identifies more therapeutic benefits of this "golden nutraceutical".⁹ At the forefront of this research, a variety of curcumin formulations have been successfully applied for the treatment of cancer cells and tumors.¹⁰ Recent work has also shown that curcumin may be used for the treatment of age-related disease.¹¹

Relevant to the modern health crisis caused by the COVID-19 pandemic, patients infected with SARS-CoV-2 who took curcumin orally exhibited significantly quicker recoveries in a double-blind, randomized trial.¹² The antiviral and antibacterial properties of curcumin have been demonstrated for other important human pathogens as well, including the influenza virus, hepatitis C virus, HIV, Zika virus, and strains of *Staphylococcus*, *Streptococcus*, and *Pseudomonas*.¹³ Curcumin acts against viruses by at least 8 distinct mechanisms: virus entry inhibition,¹⁴⁻²⁰ particle production inhibition,²¹ replication inhibition,²²⁻²⁴ cccDNA inhibition,^{25,26} protease inhibition,²⁷ integrase inhibition,²⁸ Tat protein inhibition,²⁹ and gene expression inhibition.^{30,31} As an antibacterial agent, curcumin acts as a growth inhibitor,³²⁻³⁶ biofilm formation inhibitor,³⁷ adhesion inhibitor,³⁸ and a Sortase A inhibitor of gram positive bacteria.³⁹ Curcumin has additionally been demonstrated to possess antifungal properties and acts by disrupting fungal plasma membranes.⁴⁰

Curcumin has dual effects on angiogenesis, or the formation of blood vessels, exhibiting both antiangiogenic and proangiogenic activities.⁴¹ The angiogenic effects of curcumin have been the subject of much study to elucidate the exact impact curcumin may have on human vascular health. On one hand, curcumin is an antiangiogenic compound by affecting the entire angiogenic process through downregulation of NF- κ B, an angiogenesis transcription factor, and VEGF, bFGF, and some MMPs, proangiogenic factors that have been linked to tumor progression.⁴² On the other hand, curcumin promotes neovascularization by upregulation of TGF-beta, which promotes wound healing in adults.^{34,43,44} Together, these findings demonstrate that curcumin possesses powerful pharmaceutical potential for balancing healthy angiogenesis, with potential applications ranging from topical burn treatment⁴⁵ to tumor inhibition.⁴⁶

Studies have also confirmed that curcumin has a regulatory effect on the gut microbiome, preventing the myriad of health issues that can arise as a result of dysbiosis.⁴⁷ Specifically, curcumin selects for beneficial bacterial strains in the gastrointestinal tract, as was recently confirmed by an *in vivo* study on duck gut microbiota.⁴⁸ Genera that are linked to diabetes and inflammation in individuals with high fat diets can similarly be counteracted by curcumin.⁴⁹ Additionally, other disorders linked to intestinal microflora can likewise be regulated by oral curcumin administration, including estrogen deficiency,⁵⁰ memory loss,⁵¹ and some cancers.⁵²

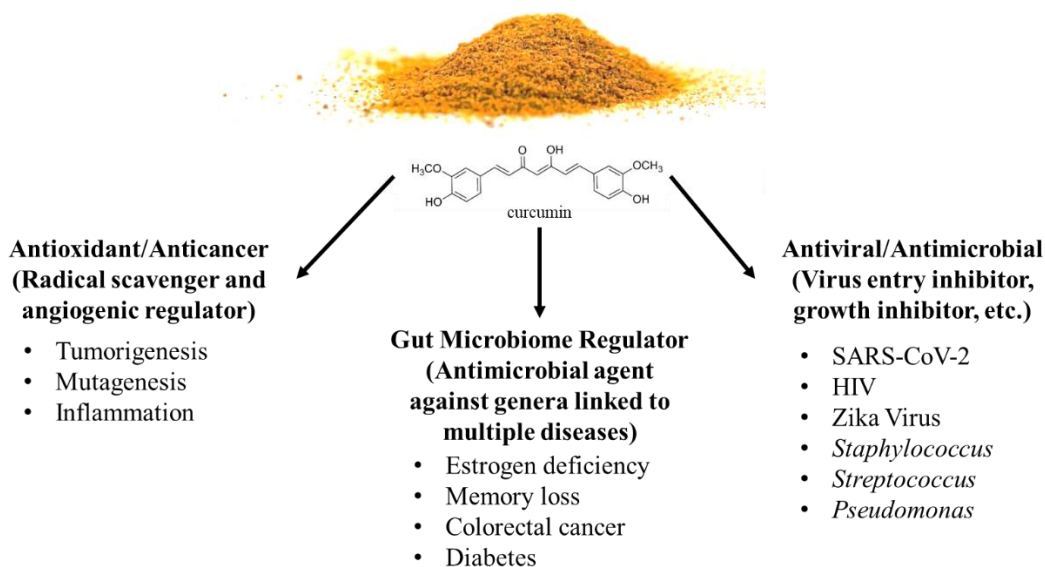


Figure 2.1: Summary of the health-promoting properties of curcumin with selected modes of action listed in parentheses and bulleted lists of target disorders being treated with curcumin formulations in clinical and academic studies.

Several curcumin products are already available on the market, including a variety of curcumin-based topical ointments which are used to reduce pain caused by inflammation of the joints, as in the case of arthritis. Bandages have also been developed with turmeric extract to promote wound healing and reduce the risk of infection. Several oral supplements are also available on the market, including curcumin nano-formulations and liposomal curcumin that are designed to enhance curcumin bioavailability.

2.2 Curcumin Production and Isolation

Curcumin is traditionally obtained using high-energy input solvent extractions from the roots of *Curcuma longa*, commonly known as turmeric spice.⁵³ Traditional extraction methods are not selective, and require the use of large amounts of toxic solvents.⁵⁴ Though much work has been done to improve the downstream processing of curcumin,⁵⁵ no amount of downstream optimization

can address the large time scale, extensive labor, and vast land required for the production of curcumin in *C. longa*.

Heterologous biosynthesis of curcumin has garnered interest in recent years as a substitute for agricultural methods. Heterologous biosynthesis addresses each of the aforementioned issues: bioreactor and fermenter footprints are on the order of square feet rather than square miles, automation has allowed most bioreactor use to require little hands-on management, and the time required to achieve biosynthetic curcumin production requires hours rather than months.⁵⁶

E. coli has been used most extensively as a host for heterologous curcumin biosynthesis.^{56–}
⁶⁰ However, recent methods have employed other hosts to attempt to improve production. One study ⁶¹ aimed to improve the malonyl-CoA supply using *Aspergillus oryzae* as the production host, with disruptions to *snfA*, which encodes an inhibitor of the acetyl-CoA carboxylase responsible to produce malonyl-CoA from acetyl-CoA, and to *SCAP*, which encodes a sterol regulatory-element binding protein cleavage-activating protein (SCAP) that utilizes acetyl-CoA for sterol biosynthesis. Together, these techniques resulted in a six-fold improvement in curcumin yield. Another study ⁶² used *Saccharomyces cerevisiae* as an engineered host for curcumin production, demonstrating that the use of a rich medium, Type III PKSs, and suppressed ferulic acid decarboxylase improved curcumin titers in the engineered strain. Most recently, the hairy roots of *Atropa belladonna*, an herbaceous plant in the nightshade family, were successfully engineered for curcuminoid biosynthesis.⁶³ The use of *A. belladonna* allowed for the synthesis of curcumin, curcumin glycosides, demethoxycurcumin and bisdemethoxycurcumin.

2.3 Heterologous Curcumin Biosynthesis in *E. coli*

The heterologous biosynthetic production of curcumin in *E. coli* can be achieved by feeding ferulic acid as a substrate, which is converted to feruloyl-CoA by a plant 4-coumarate-CoA ligase (4CL).⁶² In almost all published literature, plant 4CLs are used for engineered curcumin biosynthesis. We propose the use of a bacterial 4CL or FCS, which may exhibit higher substrate specificity toward ferulic acid based on its name and function. Subsequently, feruloyl-

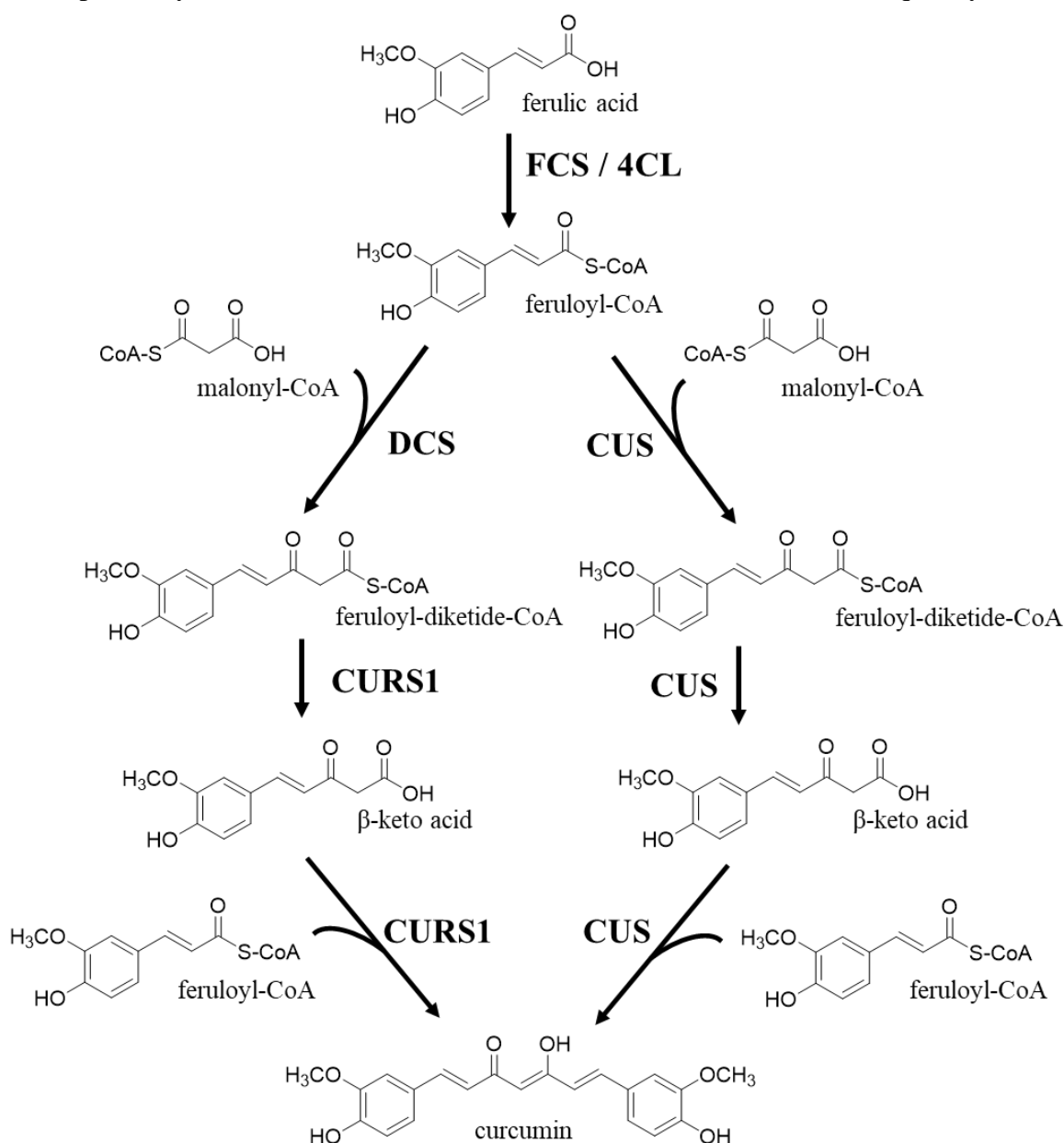


Figure 2.2: Two enzymatic approaches for achieving curcumin biosynthesis from ferulic acid.

CoA is condensed with malonyl-CoA to form feruloyl-diketide-CoA either by diketide-CoA synthase (DCS) or curcuminoid synthase (CUS). Two more condensation steps take place to form curcumin by the action of either curcumin synthase (CURS1) or again by the curcuminoid synthase (CUS)^{53,55,56,64} (**Fig. 2.2**). The conversion of ferulic acid to feruloyl-CoA may be alternatively catalyzed by a feruloyl-CoA synthase (FCS), which is often observed in the vanillin biosynthetic pathway. To our knowledge, no studies have been done to compare the efficiency of a bacterial FCS or 4CL for curcumin biosynthesis against the plant 4CL currently in use for this pathway. Specifically, the 4CL from *Arabidopsis thaliana* (4CL1) is most used for completing the reaction in most published literature. In addition, no direct comparisons have been reported for the use of DCS/CURS1 as opposed to CUS alone.

Other studies have also utilized tyrosine, coumaric acid, or caffeic acid as a starter substrate for achieving curcumin biosynthesis.^{64,65} These approaches require more enzymatic steps to form curcumin, namely the use of tyrosine ammonia lyase (TAL) to convert tyrosine into coumaric acid, 4-coumarate 3-hydroxylase (C3H) to convert coumaric acid into caffeic acid, and caffeic acid O-methyltransferase (COMT) to convert caffeic acid into ferulic acid.⁶⁶ In addition, each of these approaches can also be used to form other medically-important curcuminoids. For example, just as curcumin can be formed enzymatically from ferulic acid; bisdemethoxycurcumin can be formed from coumaric acid, dicyclopentylmethane from caffeic acid, and dicinnamoylmethane from cinnamic acid⁶⁷ (**Fig. 2.3**). Several of these curcuminoids and others have also been demonstrated to exhibit powerful activities benefitting human health.⁶⁸

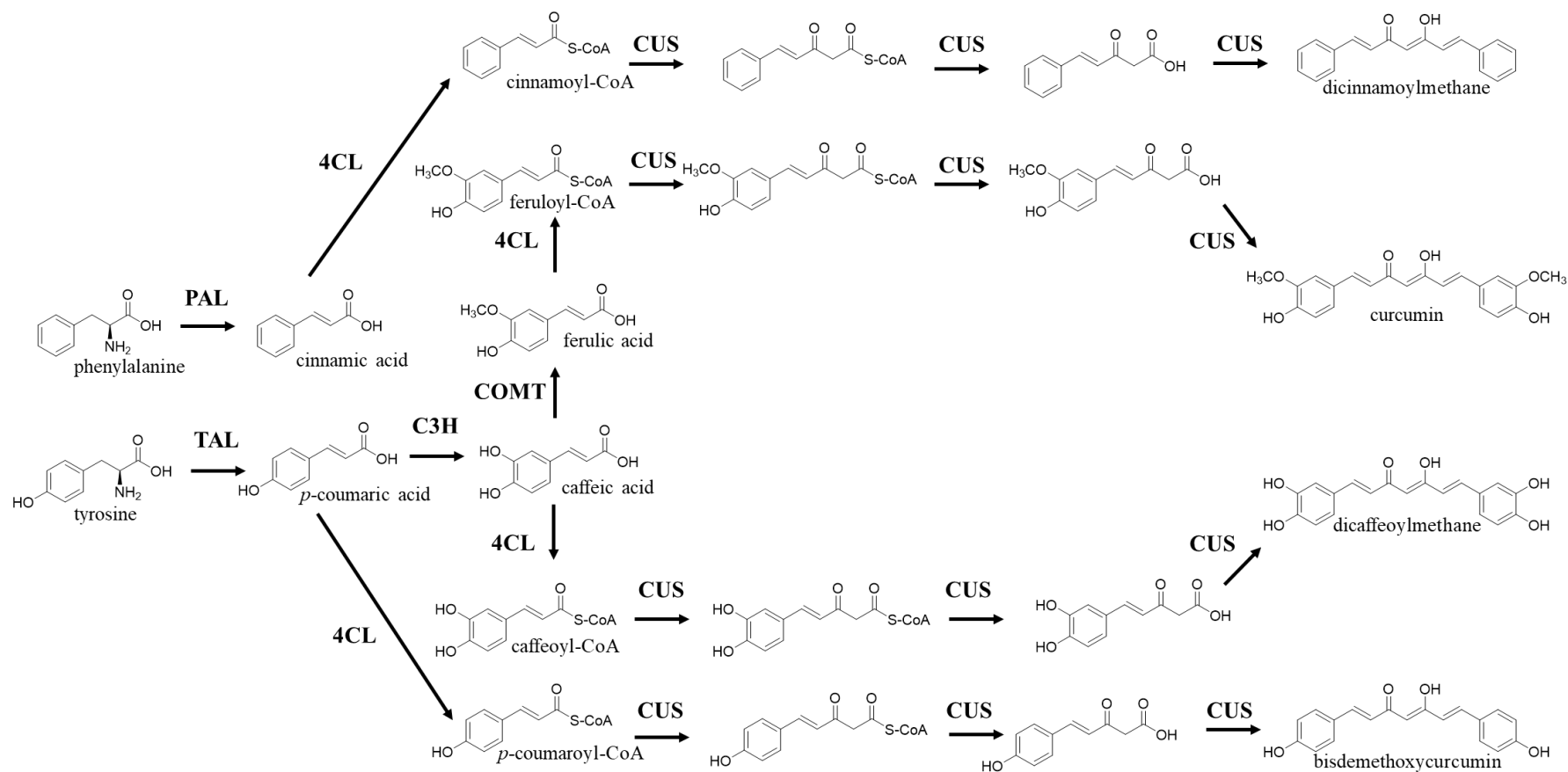


Figure 2.3: Production of various curcuminoids from amino acid precursors

Recent work has aimed to improve curcumin yields from heterologous systems by optimizing the culture medium, expression host, carbon source concentration, and induction parameters.⁵⁶ In addition, co-culture systems have been employed to improve curcumin formation by reducing the overall metabolic burden imposed on *E. coli* due to protein overexpression.⁶⁴ These efforts have resulted in markedly improved curcumin yields but have not made clear comparisons on the benefits of one enzymatic approach over another. Characterization of the alternative enzymes that can be used in the curcumin biosynthetic pathway and a clear comparison of their corresponding yields is needed to further contribute to the commercial relevance of biosynthetic methods.

2.4 Curcumin Hydrophobicity and Cytotoxic Effect on Production Host

Curcumin is a hydrophobic compound that cannot easily traverse cell membranes,⁶⁹ causing it to be mostly accumulated intracellularly in an engineered *E. coli* system.^{65,70} Some metabolic engineering methods have been employed to facilitate the intracellular storage of hydrophobic compounds such as curcumin,⁵⁸ but little work has been done to investigate methods for exporting curcumin from the cell.

The intracellular accumulation of curcumin in the engineered *E. coli* system poses an issue for cell survival, since curcumin has been shown to have an apoptotic-like effect on *E. coli*.^{71,72} This effect reduces the number of cell factories available for producing curcumin, in turn reducing the overall efficacy of the engineered system. Additionally, intracellular curcumin accumulation of *E. coli* can greatly increase the downstream processing needed for product isolation due to the need for cell disruption.⁷³ Furthermore, excretion of curcumin from the cell could allow for the use of continuous fermentation instead of batch or fill-and-draw operations. Continuous

fermentation has long been preferred over other fermentation methods and offers numerous advantages, including: (1) reduced operating costs, (2) easier operational control, (3) yield improvement, and (4) improved product consistency, among others.⁷⁴

Glycosylation is a common method utilized for improving the solubility of natural products, including curcumin.⁷⁵ Curcumin that was O-methyl-glycosylated in an *in vivo* using the fungal strain *Beauveria bassiana* ATCC 7159 exhibited a 39,000-fold improvement in water solubility over unmodified curcumin.⁷⁶ Our group recently reported the discovery and characterization of two transferases that were demonstrated to be capable of appending sugar moieties to curcumin *in vitro*, namely a glucosyltransferase from the filamentous fungus *Beauveria bassiana* ATCC 7159 (BbGT) and a UDP-glucuronyltransferase from *Streptomyces chromofuscus* ATCC 49982 (UGT).^{77,78} These enzymes are perfect candidates for testing *in vivo* glycosylation of curcumin as a method of excreting curcumin from the cell.

Similar to glycosylation, the addition of sulfate to curcumin greatly enhances its water solubility and bioavailability.⁷⁹ In human metabolism, curcumin sulfation has been demonstrated to enhance curcumin's ability to permeate the cell membrane, resulting in greatly reduced intracellular concentrations and higher curcumin titers in the culture media.⁸⁰ This detoxification mechanism allows the cell to control the overaccumulation of curcumin inside the cell. However, to our knowledge, sulfation of curcumin has yet to be employed in an engineered *E. coli* system to test its effect on engineered curcumin biosynthesis and excretion.

CHAPTER III

Experimental Methods

3.1 Genomic DNA Extraction

Various microbial hosts were screened for putative CoA-ligases from NCBI GenBank. Four hosts were selected that contained putative FCS- or 4CL-encoding genes, including *Acinetobacter* sp. NRRL B-65365, *Bradyrhizobium japonicum* USDA 6, *Bradyrhizobium diazoefficiens* USDA 110, *Photorhabdus luminescens* DSM 3368, and *Streptomyces coelicolor* A3(2). These strains were kindly provided by the USDA Agricultural Research Service Culture Collection (NRRL), except *P. luminescens* DSM 3368, which was obtained from the German Collection of Microorganisms and Cell Cultures GmbH. The gene loci for each of these genes is provided in Table 3.1.

Table 3.1: Gene loci and corresponding protein accession numbers of the CoA-ligase genes used in this study.

Putative Gene Function	Host	Gene Locus	GenBank Accession No.
feruloyl-CoA synthase	<i>Acinetobacter</i> sp. NRRL B-65365	81081...82958	LRPD01000078.1
feruloyl-CoA synthase	<i>B. japonicum</i> USDA 6 (NRRL B-4507)	8788704...8790587	AP012206.1
feruloyl-CoA synthase	<i>B. diazoefficiens</i> USDA 110 (NRRL B-4361)	476513...478369	CP011360.1
feruloyl-CoA synthase	<i>B. diazoefficiens</i> USDA 110 (NRRL B-4361)	7919197...7921080	CP011360.1
long chain fatty acid-CoA ligase	<i>P. luminescens</i> DSM 3368	829567...831255	JXSK01000001.1
acyl-CoA synthetase	<i>S. coelicolor</i> A3(2)	2622582...2624036	AL645882.2

The genomic DNA (gDNA) from each of the hosts were obtained using a phenol extraction method. First, each strain was cultivated in 4 mL of the appropriate medium as displayed in Table 3.2 below.

Table 3.2: Culture media used for obtaining gDNAs

Host	Culture Medium
<i>A. aldaricivorans</i> NRRL B-65365	Tryptone-Yeast Extract Glucose (TGY)
<i>B. japonicum</i> NRRL B-4507	Modified Arabinose Gluconate (MAG)
<i>B. japonicum</i> NRRL B-4361	Modified Arabinose Gluconate (MAG)
<i>B. japonicum</i> NRRL B-4361	Modified Arabinose Gluconate (MAG)
<i>P. luminescens</i> DSM 3368	Yeast-Malt Extract (YM)

Each culture was then pelleted and washed with Tris-EDTA (TE) buffer. Phenol and chloroform extractions were used to remove impurities and aggregate cell lysate at the interface, and each time the aqueous phase (gDNA-containing) was collected until pure gDNA was obtained, which was confirmed by gel electrophoresis using agarose gels containing ethidium bromide for visualization of DNA by UV-Vis excitation.

3.2 Identification and Cloning of Putative FCS Genes from Various Hosts

The target genes were cloned using the polymerase chain reaction (PCR) with primers designed to probe for the genes of interest. The sequences for each of the primers used are displayed in Table 3.3. The general reaction scheme for this process is shown in Table 3.4. The primers were ordered from Thermo Scientific and dissolved in Tris-EDTA (TE) buffer to the concentration of 100 ng/mL. Phusion High-Fidelity DNA polymerase was purchased from New England Biolabs. PCR was conducted with an Arktik Thermal Cycler (Thermo Scientific).

Table 3.3: Primers and plasmids used in this thesis

Gene name	Primers
65365 <i>tfcs</i> -F- <i>Nde</i> I	5'-ATCGCATATGAAAGAAATGCAAATGAATGC-3'
65365 <i>tfcs</i> -R- <i>Pac</i> I	5'-ATCGTTAATTAATTATTGCTTTAAGGTGGGCAC-3'
USDA6 <i>tfcs</i> -F- <i>Nde</i> I	5'-ATCGCATATGAGCGGACAGCCGTCCTCTTC-3'
USDA6 <i>tfcs</i> -R- <i>Kpn</i> I	5'-ATCGGGTACCTTACCCGACCGATATCACACGGTCTG-3'
4361 <i>tfcs</i> 1-F- <i>Nde</i> I	5'-ATCGCATATGACAGCCGCCTTACGCGGTGACG-3'
4361 <i>tfcs</i> 1-R- <i>Pac</i> I	5'-ATCGTTAATTAATCACCCGACGCACCCAATCCAC-3'
4361 <i>tfcs</i> 2-F- <i>Nde</i> I	5'-ATCGCATATGAATGCACAGCCGTCCTCTTCC-3'
4361 <i>tfcs</i> 2-R- <i>Pac</i> I	5'-ATCGTTAATTAATTAGCCGACCGATATCACACG-3'
3368 <i>stlB</i> - <i>Nco</i> I- <i>Nde</i> I-F	5'-TTAACCATGGGCCATATGTTGGAGAAAGTCTGGCTAAAAC-3'
3368 <i>stlB</i> - <i>Xho</i> I-R	5'-AATTCTCGAGTCAGGCTACAGCTACATTCCTGACC-3'
<i>dcs</i> - <i>Nde</i> I-F	5'-ATCGCATATGGAAGCAAATGGTTATCG-3'
<i>dcs</i> - <i>Bam</i> HI-R	5'-ATCGGGATCCTTAATTCAGACGGCAGCTATG-3'
Plasmid	Description
pJET1.2	Cloning vector
pET28a(+)	Expression vector
pACYCDuet-1	Expression vector
pCDFDuet-1	Expression vector
pET-16b	Expression vector
pSW54	<i>4cII</i> in pACYCDuet-1
pSW24	<i>cus</i> in pET28a(+)
pFZ4	3368 <i>stlB</i> in pJET1.2
pJZ164	<i>ScMatB</i> in pET28a(+)
pCB7	65365 <i>tfcs</i> in pJET1.2
pCB8	65365 <i>tfcs</i> in pACYCDuet-1
pCB9	4361 <i>tfcs</i> 1 in pJET1.2
pCB10	4361 <i>tfcs</i> 1 in pACYCDuet-1
pCB11	4507 <i>tfcs</i> in pJET1.2
pCB12	4507 <i>tfcs</i> in pACYCDuet-1
pCB13	4361 <i>tfcs</i> 2 in pJET1.2
pCB14	4361 <i>tfcs</i> 2 in pACYCDuet-1
pCB19	<i>4cII</i> from pSW54 in pET28a(+)
pCB20	4507 <i>tfcs</i> in pET28a(+)
pCB21	<i>HoST</i> in pET-16b
pCB22	Codon-optimized <i>dcs</i> -containing fragment synthesized by GeneUniversal
pCB23	<i>stlB</i> from pFZ4 in pACYCDuet-1
pCB24	Codon-optimized <i>dcs</i> in pJET1.2
pCB25	Codon-optimized <i>dcs</i> in pET-16b
pCB26	Codon-optimized <i>cursI</i> in pET28a(+)
pCB27	<i>cus</i> in pCDFDuet-1
pCB28	<i>ScMatB</i> from pJZ164 in pACYC-Duet1

Table 3.4: General PCR Reaction Scheme

Sterilized ddH ₂ O	14.2 μ L
High fidelity buffer	4.0 μ L
DMSO	0.6 μ L
100 mmol dNTPs	0.4 μ L
Forward primer	0.2 μ L
Reverse primer	0.2 μ L
Genomic DNA template	0.2 μ L
Phusion DNA polymerase	0.2 μ L
Total Volume	20 μL

3.3 Plasmid Construction, Transformation, and Purification

Cloning plasmids for each PCR product were constructed by purifying the blunt-ended PCR product using the GeneJET PCR purification kit (Thermo Scientific, USA). The purified PCR product was ligated to pJET1.2/blunt (Thermo Scientific, USA) using the ligation reaction scheme shown in Table 3.5.

Table 3.5: Ligation Reaction Scheme

pJET1.2/blunt vector	0.3 μ L
Purified PCR product	8.0 μ L
10X T4 DNA Ligase Buffer	1.0 μ L
T4 DNA Ligase	0.7 μ L
Total Volume	10 μL

Following ligation, plasmids were transformed into *E. coli* XL-1-blue using CaCl₂ chemical competent cells with heat shock, and the resulting transformation mixture was plated on LB-agar plates containing the appropriate antibiotic selection marker. Overnight incubation at 37°C allowed for the formation of visible colonies, which were picked into 4 mL liquid cultures for outgrowth at 37°C and 250 rpm for 16 hours.

Plasmids were purified from the 4 mL liquid cultures using the GeneJET Plasmid Purification Kit following the manufacturer's protocol. Plasmids were then visualized by gel electrophoresis using agarose gels containing ethidium bromide for visualization by UV excitation. Plasmids were confirmed first by restriction digest using the appropriate restriction endonucleases to excise the insert, and in cases where function was not able to be confirmed phenotypically, plasmids were sequenced to confirm the insert was correct.

In the case of pCB21, pCB22 and pCB26, plasmids were directly synthesized by Gene Universal with codon-optimized inserts for bacterial expression. pCB22 synthesis was not successfully completed and was therefore used as the PCR template for obtaining the codon-optimized *dcs* gene for amplification. The PCR product was ligated into pJET1.2/blunt, giving rise to pCB24, and the gene was then cloned into pET-16b for expression (pCB25). A summary of all plasmids is shown in Table 3.3 above.

3.4 Induction of Expression

Expression systems were developed using co-transformation by electroporation. Electrocompetent *E. coli* cells were prepared using ddH₂O and 10% glycerol (v/v) washes to remove any salts. Electro-transformation of 2-4 plasmids was achieved using a 2.5 kV pulse applied over 5 msec. Immediately after the pulse, the cells were recovered in 1mL LB broth and cultured at 37°C and 250 rpm for 1 hour. The resulting transformation mixture was plated on LB-agar plates containing the appropriate antibiotic selection markers corresponding to the co-transformed plasmids. Incubation overnight at 37°C facilitated the formation of visible colonies, which were picked into 4 mL liquid seed cultures. The 4 mL TB seed cultures were then outgrown for 16 hours at 37°C and 250 rpm.

After outgrowth, flasks containing 50 mL TB and the working concentration of the appropriate antibiotics were inoculated using 1% v/v seed culture. The cultures were grown to an $OD_{600} = 0.7 - 0.9$, and expression was induced by the addition of 0.1 mM IPTG after cooling the cultures to 4°C. The cultures were then transferred to a 28°C and 250 rpm incubating shaker for expression. Five hours following the addition of IPTG, 2 mM ferulic acid and 1% v/v glycerol were added as substrates, and biotransformation of ferulic acid to curcumin was allowed to proceed for 63 hours post-induction.

3.5 Enzyme Purification and Kinetic Assays

The *At4cl1* gene was cloned into pET28a(+) between NdeI and XhoI restriction sites (pCB19) for expression of a His₆-tag fusion protein, and *4507fcs* genes was likewise cloned between NdeI and HindIII restriction sites (pCB20). For expression, 200 mL LB cultures in 1 L flasks containing kanamycin (50 µg mL⁻¹) were inoculated with 1% v/v overnight seed cultures and grown to an OD_{600} of 0.4 - 0.6. Protein expression was induced after cooling to 4°C by the addition of 200 µM IPTG, and the flasks were transferred to incubators at 18°C and 250 rpm for around 20 hours. The cultures were then pelleted by centrifugation at 3,000 × g and 4°C for 10 min and resuspended in cold lysis buffer (20 mM Tris-HCl buffer (pH 7.9) and 0.5M NaCl with 1 mM dithiothreitol). Cell disruption was achieved using ultrasonication (Misonix Sonicator 3000, Misonix Inc., USA) on ice. The lysate was centrifuged at 10,000 × g and 4°C for 10 min to collect the soluble fraction containing the target proteins which was analyzed by sodium dodecyl sulfate-polyacrylamide gel electrophoresis (SDS-PAGE). SDS-PAGE analysis used a pre-stained protein ladder (EZ-Run™ Pre-Stained Rec Protein Ladder, molecular range: 11-170 kDa, Fisher BioReagents) as the reference. After electrophoresis, the gel was stained with 0.1% Coomassie Brilliant Blue R250, and destained in 20% (v/v) acetic acid-water.

Enzyme purification was achieved by binding the supernatant from the cell lysates onto a HisPur™ Ni-NTA agarose affinity column (Thermo Scientific, Rockford, USA) according to the manufacturer's protocol. The column was washed with cold (4°C) washing buffers (50 mM Tris-HCl, 2 mM EDTA, 10 mM, 25 mM, and 250 mM imidazole, pH 7.9) and the recombinant proteins were concentrated from the 25 mM and 250 mM imidazole fractions by buffer A (50 mM Tris-HCl, 2 mM EDTA, pH 7.9) using the 30,000 MWCO Macrosep Advance Centrifugal Device (Pall Corporation, New York, USA). The enzymes were suspended in 50% glycerol (v/v) and stored at -20°C. The protein concentration was determined using the Bio-Rad Quick Start™ Bradford Protein Assay (Hercules, CA, USA) following the manufacturer's protocol.

Enzyme kinetics assays were performed for both At4CL1 and 4507FCS purified enzymes. The reaction mixture (500 µL) contained 5 µg purified protein, 7 mM CoA, and 2 mM ATP in 100 mM potassium phosphate buffer. Ferulic acid was also present in concentrations ranging from 0.1 – 6.6 mM. The reaction was initiated by the addition of 5 µg enzyme and was incubated at room temperature for 20 minutes. The reaction was quenched using 1 mL methanol, and all 1.5 mL of the reaction mixture was loaded to a clean 1 cm cuvette. Change in absorbance at 345 nm was used to quantify the formation of feruloyl-CoA using the reported molar absorptivity of feruloyl-CoA of 19,000 M⁻¹ cm⁻¹.⁸¹ The resulting concentration of feruloyl-CoA was then calculated using the Beer-Lambert law. Since both enzymes exhibited Michaelis-Menten kinetic behavior, kinetic parameters were determined by plotting the data on a double-reciprocal (Lineweaver-Burke) plot.

3.6 Product Isolation and Quantification

Curcumin titer was quantified using a whole broth concentration method. Briefly, 2 mL of well-mixed whole broth were dried under reduced pressure and recovered in 1 mL 50/50 dimethyl sulfoxide-methanol. Sonication homogenized the concentrated whole broth and facilitated cell

lysis, and the resulting sample was centrifuged at 15,000 rpm for 10 minutes in preparation for HPLC analysis. From the supernatant, 100 μ L were injected to HPLC and subjected to chromatographic and UV-Vis absorbance analysis. Curcumin was detected using a 420 nm wavelength and eluted at 28 min when operating in gradient mode with methanol-water as the mobile phase (5:95 to 95:5 over 35 min, v/v, containing 0.1% formic acid) with a 1 mL/min flow rate. ESI-MS spectra were acquired using an Agilent 6130 single quadrupole LC-MS system in the negative mode to confirm the molecular weights of the curcuminoid products, except for dicinnamoylmethane, which was confirmed by ESI-MS operating in the positive mode due to its chemical structure.

For experiments comparing the intracellular and extracellular yields, the whole broth concentrates (CWB) were obtained together with cell-free fermentation broth concentrates (CFB). CWB samples were used to determine the total curcumin yield, while CFB samples represented the extracellular curcumin yield. The “extracellular fraction” of curcumin was determined using the simple equation:

$$\text{Extracellular Fraction} = \frac{\text{CFB Titer} \left[\frac{\text{mg}}{\text{L}} \right]}{\text{CWB Titer} \left[\frac{\text{mg}}{\text{L}} \right]}$$

The CFB samples were obtained by centrifuging all 50-mL culture at 3,500 rpm for 5 minutes to pellet the cells, and 4 mL of the resulting supernatant were dried under reduced pressure and recovered in 1 mL of 50/50 dimethyl sulfoxide-methanol. As before, the samples were sonicated and spun in preparation for HPLC, where 100 μ L of the final supernatant were loaded to HPLC for analysis.

3.7 Statistical Methods

In the case of all yield experiments, samples were collected in triplicate for each treatment group. The data were fitted with one-way ANOVA using the SAS On Demand online environment. Pairwise comparisons were made between each treatment group using the Tukey-Kramer adjustment to control the family-wise error rate, or, as appropriate, comparisons were only made against the control using the Dunnett's adjustment. Differences were considered significant only for $p < 0.05$ in all cases. Response variables are reported as mean titer \pm standard deviation (SD) in mg L^{-1} .

CHAPTER IV

Results

4.1 Identification of an Efficient FCS from *Bradyrhizobium japonicum* USDA 6

Screening of various putative CoA-ligases showed that several indeed encode functional proteins exhibiting feruloyl-CoA synthase (FCS) activity. Functional screening was confirmed by co-expression of the putative CoA-ligase-encoding plasmid with pSW24 that harbors the curcuminoid synthase (CUS). Curcumin formation was obvious based on the yellowing of the culture broth, and HPLC analysis confirmed the presence of curcumin in several samples. Only pCB28, encoding ScMatB, did not show any FCS activity. The native function of ScMatB is to

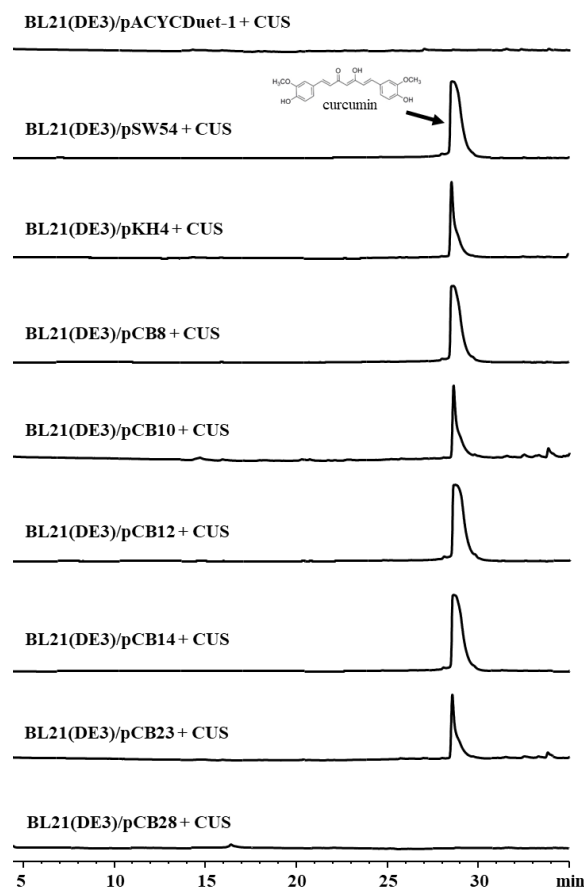


Figure 4.1: HPLC analysis using 420 nm to detect the formation of curcumin when each FCS-encoding construct was co-expressed with CUS. pACYCDuet-1 served as a negative control, and pSW54 served as the positive control.

convert malonate to malonyl-CoA, so the lack of substrate flexibility toward ferulic acid is likely due to the phenolic ring causing steric hindrance in the active site of ScMatB. Stacked HPLC chromatograms compared to a negative control (blank pACYCDuet-1 + pSW24) and a positive control (pSW54 + pSW24) are displayed in Figure 4.1.

In the interest of making a statistically relevant yield comparison between each of the functional FCSs, expressions were performed in triplicate for each under the same expression conditions as before. Comparisons were made for each “high productivity” FCS-encoding plasmid against pSW54 (encoding At4CL1 commonly used for heterologous curcumin biosynthesis). High productivity FCSs were determined loosely based on peak area and included the FCSs encoded in pCB8, pCB12, pCB14, and pKH4. The results revealed that the FCS encoded in pCB12 (the FCS from *B. japonicum* USDA 6 B-4507) could potentially improve yield compared to At4CL1, improving the yield from $13.99 \pm 0.67 \mu\text{g/mL}$ to $17.37 \pm 3.23 \mu\text{g/mL}$ (Fig. 4.2).

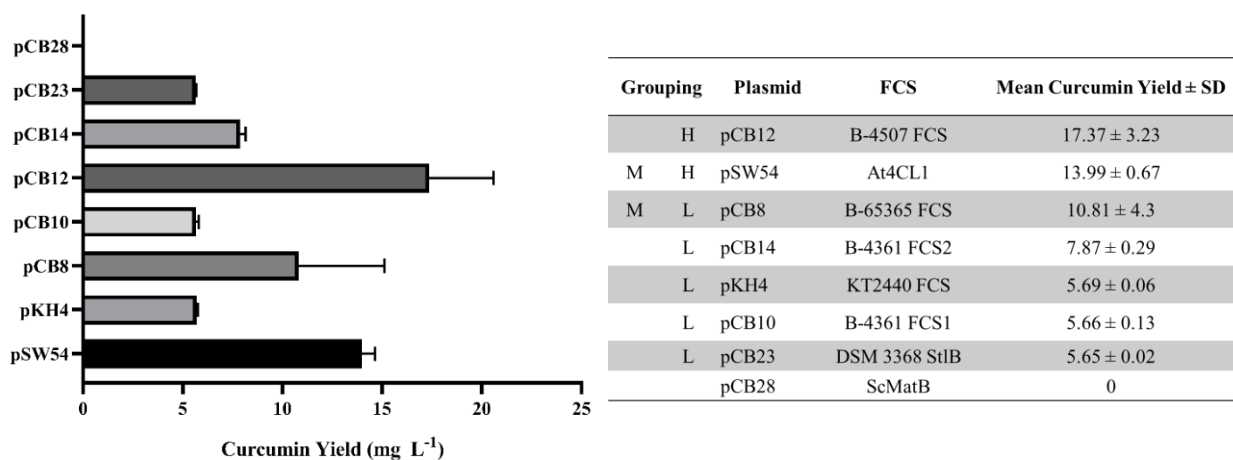


Figure 4.2: Curcumin yield comparisons of each FCS. Left: Bar graphs showing mean curcumin production \pm SD for each FCS in mg L^{-1} . Right: Statistical grouping (Tukey-Kramer) of FCSs based on curcumin yield. H indicates high productivity, M indicates moderate productivity, and L indicates low productivity. FCSs with the same grouping are not significantly different from each other at the $p < 0.05$ significance level.

Though the difference between 4507FCS and At4CL1 was not significantly different, 4507FCS was the only FCS categorized solely as a “high” curcumin producer, encouraging us to further investigate this enzyme for use in the curcumin biosynthetic pathway. We hypothesize that since 4507FCS is a dedicated bacterial enzyme, it may exhibit improved enzymatic activity over the plant At4CL1 in a bacterial production system. It is important to mention that the overall curcumin yield was low, as is common when using CUS as the condensing enzyme in the biosynthetic pathway.⁶⁵

4.2 Kinetic Parameters of 4507FCS v. At4CL1 *in vitro*

Due to the observed increase in yield using 4507FCS compared to At4CL1, we were encouraged to isolate these enzymes for *in vitro* kinetic analysis. Each enzyme was successfully purified to near homogeneity by Ni-NTA Agarose resin column chromatography using increasing concentrations of imidazole in the mobile phase. The purified proteins were then confirmed by loading 1 μ L of the pure enzyme stock to SDS-PAGE. Both purified proteins were approximately 70 kDa in size (Fig. 4.3).

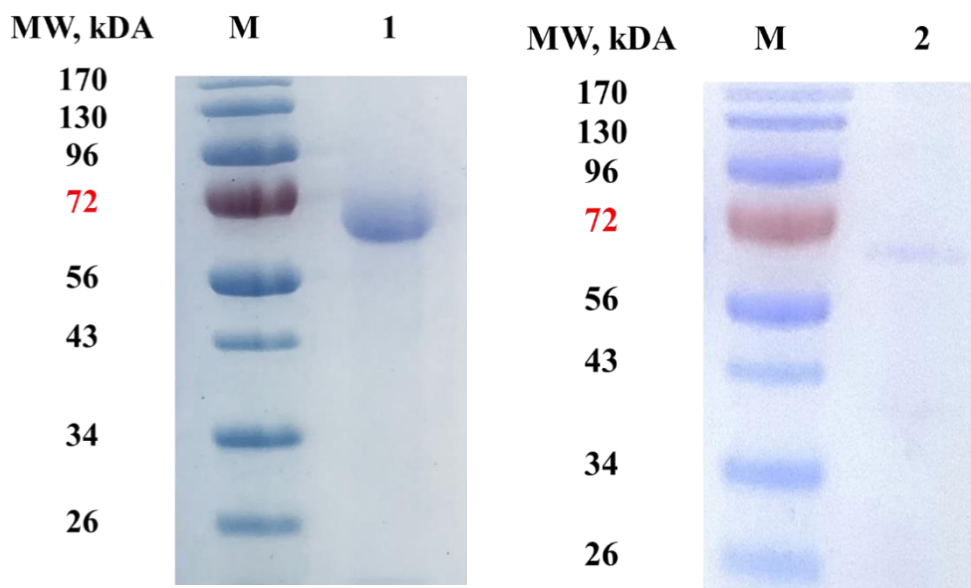


Figure 4.3: SDS-PAGE analysis of purified At4CL1 (1) and 4507FCS (2) compared to protein standards (M).

Based on the SDS-PAGE results, At4CL1 had substantially better expression over 4507FCS. The isolated yields were calculated for each enzyme using a Bradford assay to make a quantitative comparison between the expression level. The stock concentrations of 4507FCS and At4CL1 were determined to be 371.0 mg L^{-1} and 6193.4 mg L^{-1} , respectively. These stock concentrations were used to determine the total protein yield from the 200 mL LB expression system, which were found to be 1.855 mg L^{-1} for 4507FCS and 30.967 mg L^{-1} for At4CL1, indicating that At4CL1 may have over 16 times higher expression levels than 4507FCS when expressed in *E. coli*.

Kinetic assays revealed that both proteins exhibited Michaelis-Menten style kinetics, allowing for the determination of the enzymatic kinetic constants by plotting the data on a double reciprocal (Lineweaver-Burke) plot (Fig. 4.4).

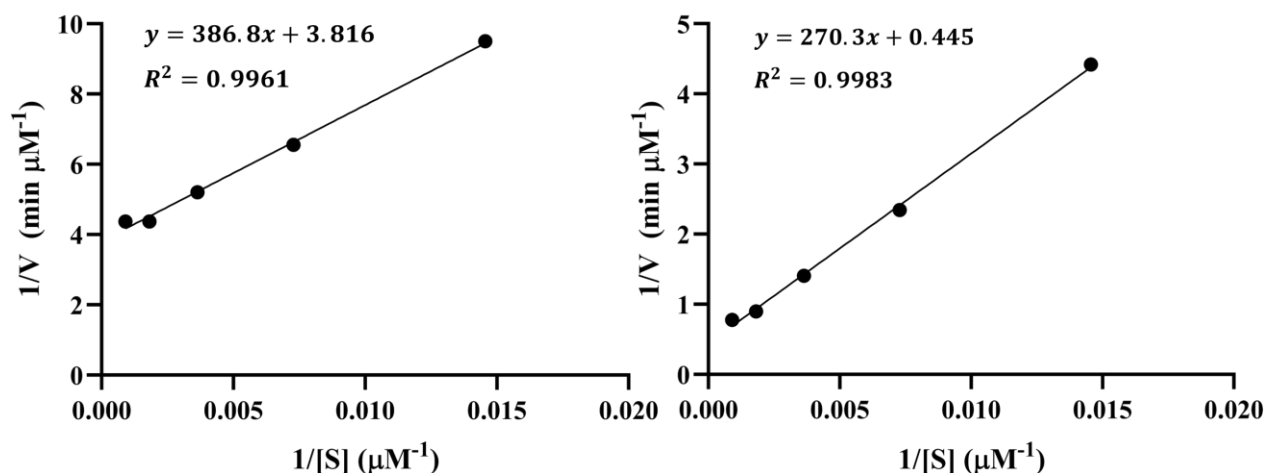


Figure 4.4: Lineweaver-Burke Plots for At4CL1 (left) and 4507FCS (right)

The linear regression data were then used to calculate the key kinetic parameters for these two enzymes, which are displayed below in Table 4.1. It was revealed that 4507FCS exhibited improved enzymatic activity over At4CL1, with a net 73% improvement in k_{cat}/K_m . Specifically, the enzyme exhibited improved catalytic efficiency, with a k_{cat} of 0.767 s^{-1} compared to the

At4CL1 k_{cat} of 0.074 s^{-1} . Interestingly, the K_m of 4507FCS was higher than that of At4CL1, suggesting that the enzyme may not be as efficient for binding the substrate under low substrate concentrations. High ferulic acid concentrations (exceeding 2 mM) have been avoided in other studies to avoid substrate toxicity to the production host, indicating that excess ferulic acid may negatively impact *E. coli*. One method to circumvent this issue is the addition of 2 mM at the beginning of the fermentation run, followed by the addition of 1mM ferulic acid 15 hours later, rather than adding all 3 mM at the beginning of the run.⁶⁴

Table 4.1: Enzyme kinetics for At4CL1 and 4507FCS

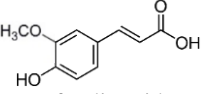
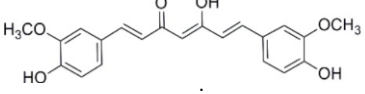
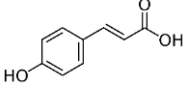
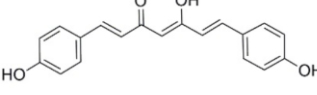
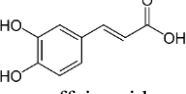
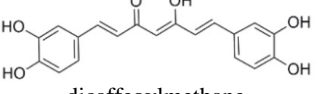
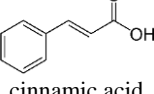
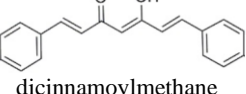
Kinetic Parameter	At4CL1	4507FCS	% Change
[E] (μM)	0.06	0.05	-
V_{max} ($\mu\text{M min}^{-1}$)	0.26	2.25	+765%
K_m (μM)	101.4	608.0	+500%
k_{cat} (s^{-1})	0.074	0.767	+936%
k_{cat}/K_m ($\text{M}^{-1} \text{s}^{-1}$)	728.3	1261.1	+73%

4.3 Investigation of StlB for Curcuminoid Production

One of the screened proteins that exhibited low FCS activities was StlB, a bacterial CoA-ligase from *P. luminescens* DSM 3368 that is involved in bacterial stilbene biosynthesis. StlB has the native function of catalyzing the conversion of cinnamic acid to cinnamoyl-CoA, which is used as a precursor for the formation of 3,5-dihydroxy-4-isopropyl-*trans*-stilbene, commonly known as Benvitimod or Tapinarof.^{82,83} To investigate the substrate flexibility of StlB for the formation of various curcuminoids, an StlB-encoding construct (pCB23) was co-transformed with pSW24, encoding CUS. Several expression cultures were used to test the effect of different substrates to screen for the formation of various curcuminoids. Based on the corresponding curcuminoids

formed, it was found that StlB exhibits strong cinnamoyl-CoA synthase activity, as well as weak FCS and *p*-coumaroyl-CoA ligase activity. However, StlB cannot take caffeic acid as a substrate for the formation of caffeoyl-CoA. A summary of the HPLC-MS data used to confirm the formation of these products is displayed in Table 4.2.

Table 4.2: Summary of StlB substrate flexibility testing. n.d. indicates no data obtained due to extremely low activity.

Substrate	StlB + CUS Product	ESI-MS Data (m/z)	At4CL1 Peak Area	StlB Peak Area	Deduced StlB CoA-Ligase Activity
 ferulic acid	 curcumin	366.9 [M-H] ⁻	43765.0	235.8	Weak
 <i>p</i> -coumaric acid	 bisdemethoxycurcumin	306.9 [M-H] ⁻	12895.1	2623.2	Weak
 caffeic acid	 dicafeoylmethane	n.d.	6106.5	n.d.	None
 cinnamic acid	 dicinnamoylmethane	277.0 [M+H] ⁺	12903.6	20948.3	Strong

Detailed chromatograms, ESI-MS spectra, and UV-Vis spectra for each of the data points contained in Table 4.2 are displayed in Appendix A.

4.4 Optimization of the Curcumin Biosynthesis Enzymatic Approach

In plants, two common biosynthetic pathways are commonly used for producing curcumin, as depicted previously in Figure 2.2. These two pathways have been studied extensively, and it is generally understood that the use of 4CL and CUS alone yields less curcumin than the 4CL, DCS, and CURS1 approach. However, no work to our knowledge has been conducted to elucidate the exact limiting step in the curcumin biosynthetic pathway. To address this issue, we used the

efficient 4507FCS identified previously, to make comparisons on four enzymatic approaches for achieving curcumin biosynthesis were evaluated for productivity. The four enzymatic approaches tested are summarized in Table 4.3.

Table 4.3: Enzymatic approaches for achieving curcumin biosynthesis investigated in this thesis.

No.	Enzyme Combination	Plasmids Used
1	FCS + CUS	pCB12 + pSW24
2	FCS + DCS + CURS1	pCB12 + pCB25 + pCB26
3	FCS + DCS + CUS	pCB12 + pCB25 + pSW24
4	FCS + DCS + CUS + CURS1	pCB12 + pCB25 + pCB26 + pCB27

Each of the enzymatic approaches was constructed by co-transformation of the appropriate plasmids and expressed in triplicate. All possible pairwise comparisons were made on the resulting yields to demonstrate which combination of enzymes provided the best curcumin yield. The average yields, reported as mean yield \pm standard deviation in mg L⁻¹, for each of the approaches are presented in Table 4.4.

Table 4.4: Mean curcumin yields for each enzymatic approach

No.	Mean Curcumin Yield \pm SD (mg L⁻¹)
1	15.5 \pm 0.7
2	104.7 \pm 12.6
3	73.0 \pm 11.1
4	118.0 \pm 1.6

There are four key findings from this experiment. First, we confirmed that the efficacy of CUS alone is far inferior to that of DCS + CURS1, as made evident by the large curcumin yield difference between approaches **1** and **2**. This comparison had generally been understood in previously reported literature, but no exact yield data had been tied to the approaches.

Second, it was found that DCS is the key determining factor for improving curcumin production in *E. coli*. This can be deduced by the significant yield improvement in the DCS-

containing combinations (2 – 4) compared to approach 1. Special interest should be placed on the large yield improvement between approaches 1 and 3, which demonstrates that the rate-limiting step in the curcumin biosynthetic pathway is the formation of feruloyldiketide-CoA from feruloyl-CoA and malonyl-CoA. Addition of DCS to approach 1 improved the yield from 15.5 ± 0.7 to 73.0 ± 11.1 mg L⁻¹, corresponding to a 4.7-fold improvement in curcumin yield.

Third, within the DCS-containing group, it was further demonstrated that CURS1 is a more efficient condensing enzyme than CUS, as made evident based on the observed increase in yield between approaches 2 and 3. The use of CURS1 improved curcumin yield from 73.0 ± 11.1 to 104.7 ± 12.6 mg L⁻¹, corresponding to a 1.5-fold improvement.

Finally, we demonstrated that the full construction of both enzymatic approaches as achieved in approach 4 further enhances the yield over approach 2 and 3. Though no significant difference was observed between approaches 2 and 4, the trend is fascinating considering the increased metabolic burden imposed on *E. coli* in approach 4 over approaches 2 or 3. These data suggest that the full construction of both pathways has a positive impact on curcumin production, as the pathways mutually build the metabolic intermediate pools.

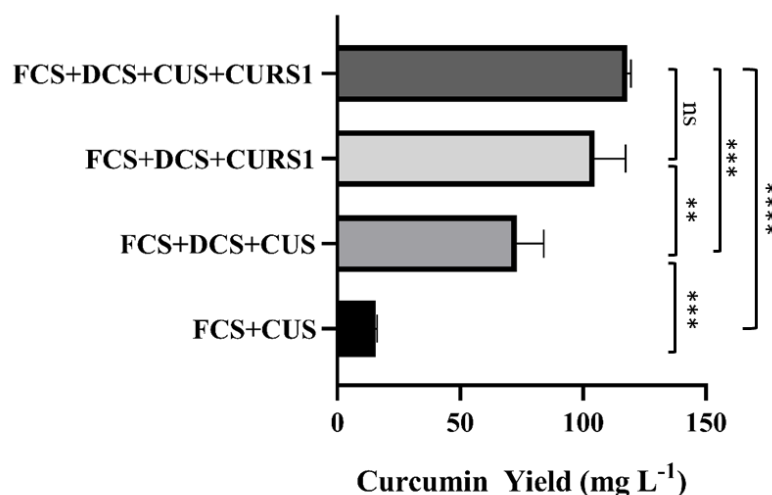


Figure 4.5: Curcumin yield comparisons for enzymatic approaches 1 through 4. **** indicates $p < 0.0001$, *** indicates $p < 0.001$, ** indicates $p < 0.01$, and ns indicates no significant difference.

Each of these comparisons and the strength of the statistical significance between each group may be visualized in Figure 4.5.

4.5 Glycosylation of Curcumin *In Vivo*

Simultaneous production and glycosylation of curcumin was performed by the co-expression of the curcumin biosynthetic enzymes encoded in pCB12 and pSW24 together with either the novel fungal glucosyltransferase (BbGT) or bacterial UDP-glucuronyltransferase (UGT), encoded in pCB15 and pCB16, respectively. Previously, when added as an exogenous substrate to the expression culture, curcumin could not be glycosylated (data not shown). We theorize that glycosylation could not occur since curcumin is practically water insoluble⁸⁴ and does not readily traverse the cell wall of *E. coli*, thus separating the curcumin substrate from the enzymes across the cell wall. Interestingly, when BbGT and UGT were co-expressed with the curcumin biosynthetic enzymes, both glucosylation and glucuronidation of curcumin were achieved, as confirmed by the formation of glucosylated and glucuronidated curcumin products.

The curcumin glucoside had a retention time of 20.5 minutes, which was 3.5 minutes earlier than curcumin, which eluted at 24 minutes using a gradient mode HPLC method with methanol-water as the mobile phase (20:80 to 95:5 over 25 min, v/v, containing 0.1% formic acid) with a 1 mL/min flow rate. The UV-Vis spectrum of the glucoside was similar to that of curcumin, which suggested that the product shared the same core structure. ESI-MS spectra has not yet been successfully captured for the glucosylated product, which is typically produced in very low titers (**Fig. 4.6**).

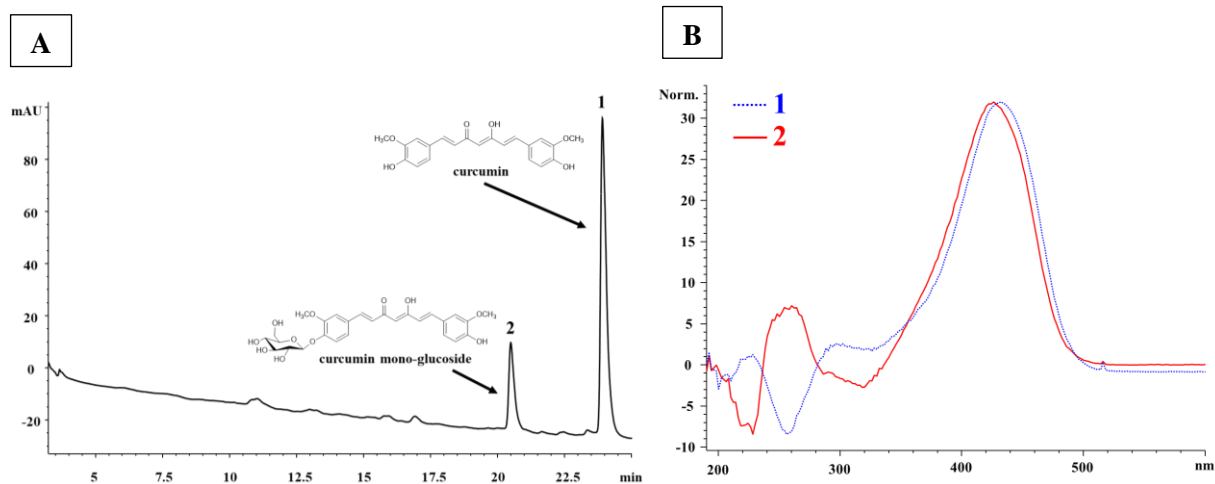


Figure 4.6: Formation of curcumin and curcumin glucoside by *E. coli* BL21(DE3) / pCB12 + pSW24 + pCB15. (A) HPLC chromatogram measuring absorbance at 420 nm, showing two peaks corresponding to curcumin (**1**) and curcumin glucoside (**2**); (B) Overlaid UV-Vis spectra of peaks **1** and **2**.

The glucuronidated curcumin product had a retention time of 12.5 minutes, suggesting an improvement in water solubility compared to curcumin, which eluted at 17 minutes. The HPLC method used a 420 nm wavelength and gradient mode operation with methanol-water as the mobile phase (45:55 to 95:5 over 25 min, v/v, containing 0.1% formic acid) with a 1 mL/min flow rate. The UV-Vis spectrum of the glucuronide was very similar to that of curcumin, suggesting similarity in core structure, and the molecular weight was confirmed by ESI-MS to be curcumin monoglucuronide based on the addition of 176 g mol^{-1} for a total mass of 544 g mol^{-1} . These data are all displayed below in Figure 4.7.

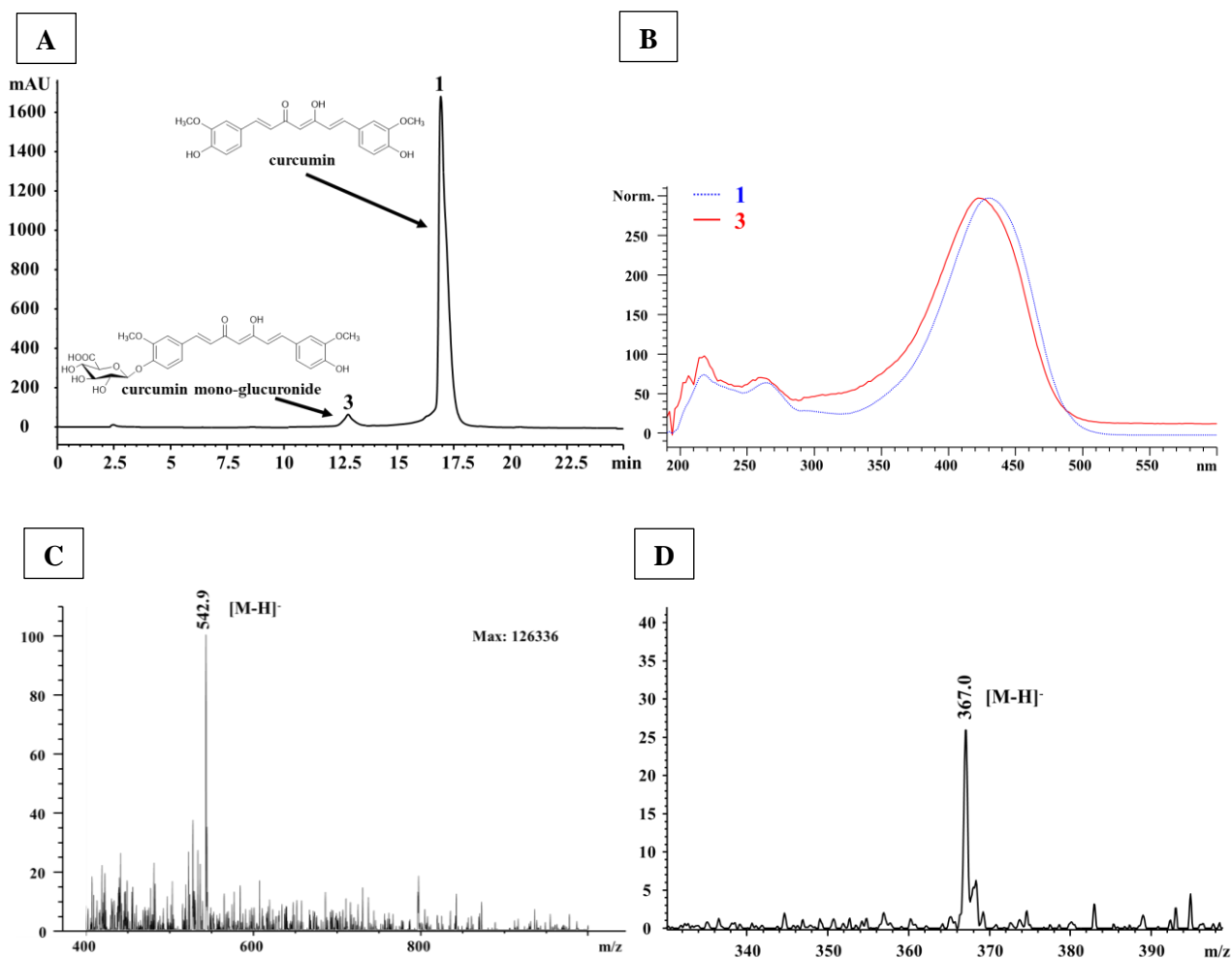


Figure 4.7: Formation of curcumin and curcumin glucuronide by *E. coli* BL21(DE3) / pCB12 + pSW24 + pCB16. (A) HPLC chromatogram showing the simultaneous production of curcumin (1) and curcumin glucuronide (3); (B) Overlaid UV-Vis spectra of peaks 1 and 3 suggest a similar core structure; (C) ESI-MS spectra for peak 3, confirming curcumin monoglucuronide product; (D) ESI-MS spectra for peak 1, confirming curcumin production.

4.6 Sulfation of Curcumin *In Vivo*

The *Haliangium ochraceum* DSM 14365 sulfotransferase (HoST) (from gene locus Hoch_5094, GenBank Accession No. CP001804.1) was selected as a target enzyme for sulfating curcumin *in vivo*. HoST was selected as a target enzyme due to its reported versatility for the sulfation of small molecules. Specifically, HoST is an aryl sulfotransferase that exhibits broad substrate specificity within the phenolic compound family and works especially well for the sulfation of symmetrical phenolics such as 4,4'-biphenol.⁸⁵ Since curcumin is also a symmetrical

biphenolic molecule, we hypothesized that HoST could be an excellent enzyme target for curcumin sulfation *in vivo*.

To determine if HoST could accept curcumin as a substrate, HoST was first expressed alone in *E. coli* BL21(DE3). The same expression conditions were utilized as with other expression experiments, but 10 mg of curcumin were supplemented as substrate 5 hours after the addition of 0.2 mM IPTG. The fermentation broth was then sampled after 24 hours of biotransformation. HPLC-MS analysis conducted on 100 μ L of cell-free fermentation broth revealed the formation of curcumin sulfate, with a molecular mass of 448 g mol^{-1} , confirmed by ESI-MS. The UV-Vis spectra of curcumin and curcumin sulfate were also highly similar, suggesting a similar molecular core structure (**Fig. 4.8**).

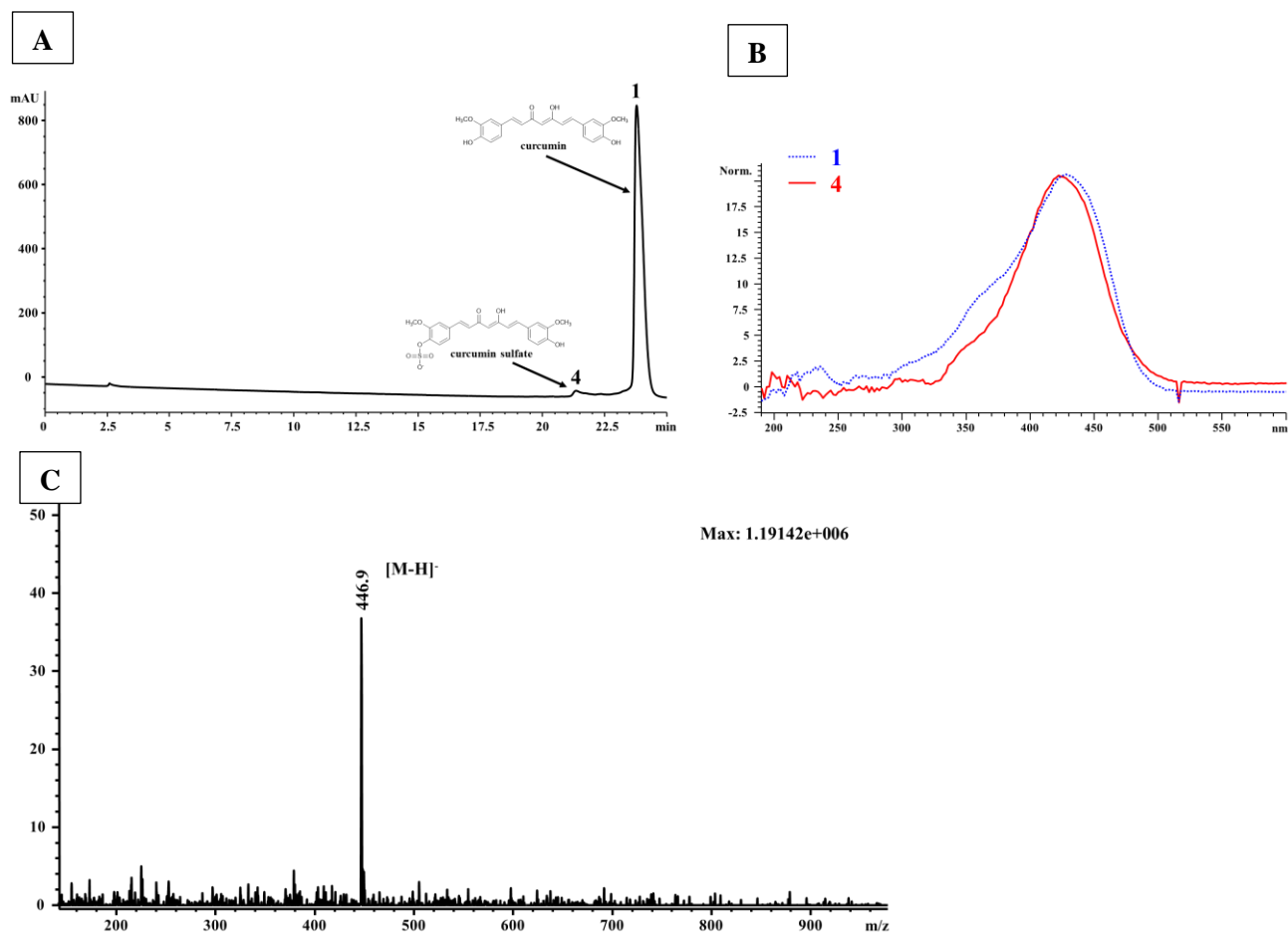


Figure 4.8: Biotransformation of curcumin into curcumin sulfate by *E. coli* BL21(DE3) / pCB21. (A) HPLC chromatogram showing the formation of curcumin (1) and curcumin sulfate (2); (B) Overlaid UV-Vis spectra of peaks 1 and 4 suggest a similar core structure; (C) ESI-MS of peak 4 demonstrates that HoST can accept curcumin as a substrate for the formation of curcumin sulfate, as indicated by the addition of 80 g mol^{-1} to curcumin (368 g mol^{-1}).

After confirming that HoST indeed accepts curcumin as a substrate, we were encouraged to attempt curcumin production with simultaneous expression of HoST to allow for sulfation of curcumin as it is produced for eventually modulating curcumin excretion. A time course experiment was conducted to identify the best biotransformation period to maximize the production of curcumin and curcumin sulfate. As might be expected, curcumin peak area decreased over time while curcumin sulfate peak area increased as curcumin was bio-transformed into its sulfated conjugate (**Fig. 4.9**).

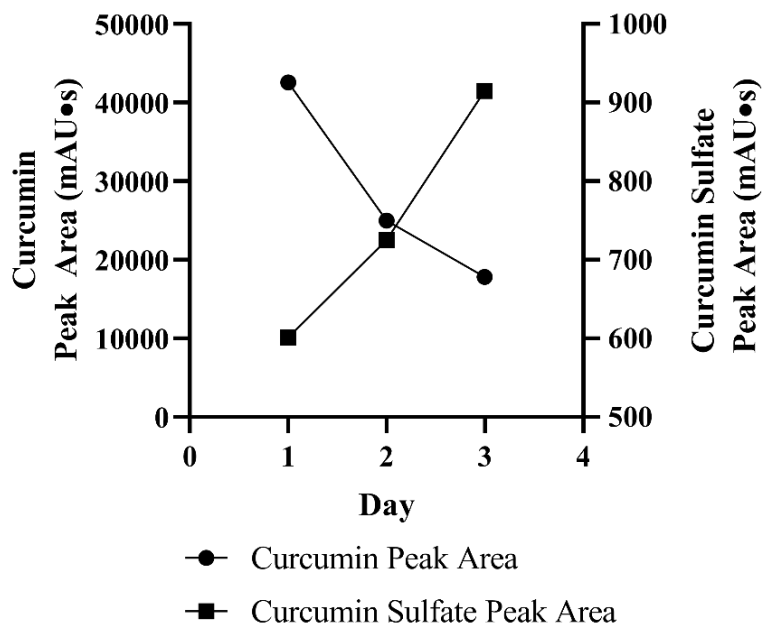


Figure 4.9: Curcumin sulfate production is inversely proportional to curcumin production over time

The sulfated product in the co-expression system exhibited a reduced retention time compared to when HoST was expressed alone. HPLC-MS analysis revealed that the co-expression sulfation product had a molecular mass of 528.3 g mol^{-1} , representing the addition of 160 g mol^{-1} to the curcumin mother structure. These data suggest that in the co-expression system, curcumin can be sulfated on both phenolic rings, likely in a stepwise fashion, to yield curcumin disulfate. The UV-Vis spectra of the di-sulfated product was not significantly different from that of curcumin, again suggesting that the core structure was preserved (**Fig. 4.10**).

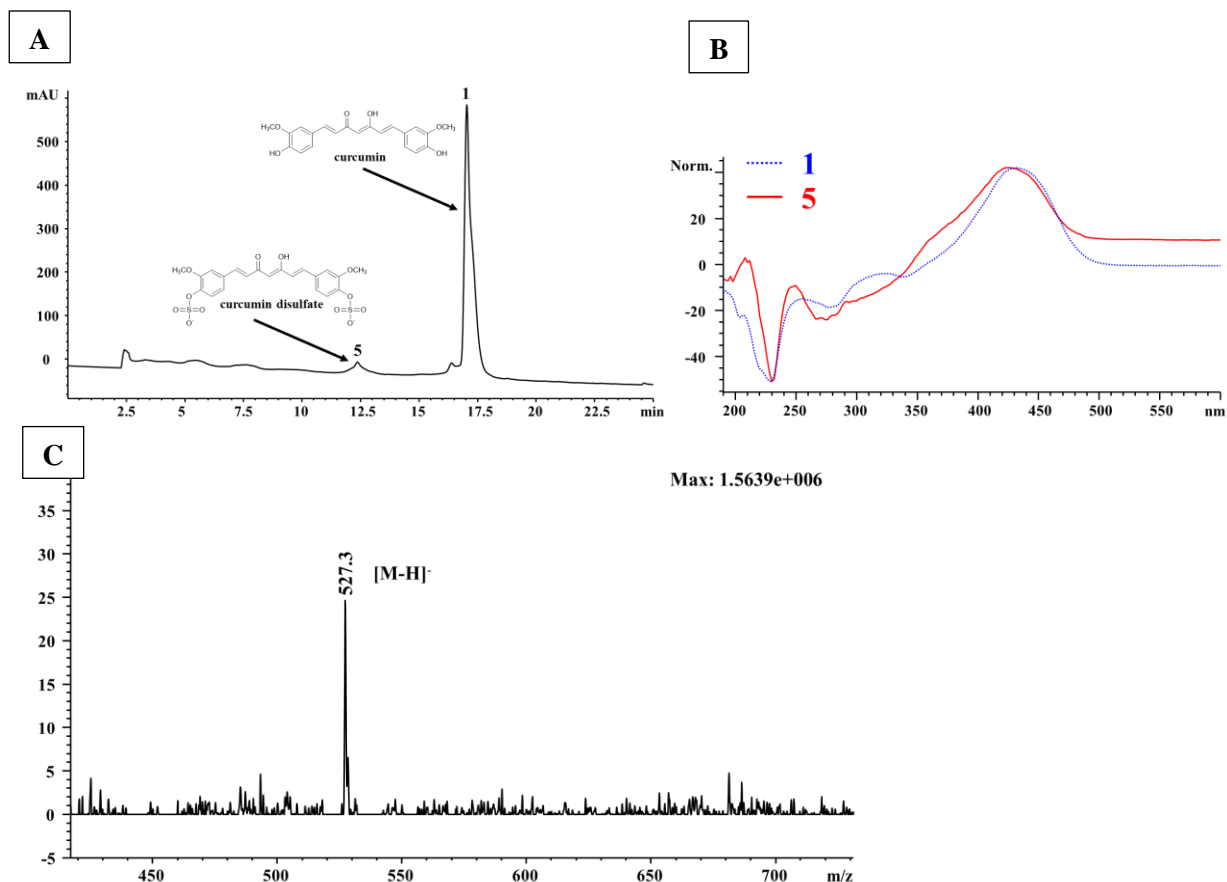


Figure 4.10: Curcumin di-sulfate was obtained when curcumin biosynthetic enzymes were co-expressed with HoST in *E. coli*. (A) HPLC chromatogram showing the retention times of curcumin (**1**) and curcumin disulfate (**5**); (B) Overlaid UV-Vis spectra of **1** and **5** demonstrate similarity, suggesting a similar core structure; (C) ESI-MS spectra of peak **5** revealed that the product was indeed curcumin disulfate.

4.7 Effect of Transferase Co-Expression on Curcumin Excretion

We next aimed to improve curcumin excretion to pave the way to continuous fermentation systems. Three transferases were investigated: a fungal glucosyltransferase from *Beauveria bassiana* ATCC 7159 (BbGT), a bacterial UDP-glucuronyltransferase from *Streptomyces chromofuscus* ATCC 49982 (UGT), and a sulfotransferase from *Haliangium ochraceum* DSM 14365 (HoST). In the interest of minimizing metabolic burden by the co-expression of several plasmid DNAs, each transferase was expressed with FCS and CUS rather than FCS, DCS, and CURS1, exchanging metabolic burden for decreased curcumin production efficiency. Triplicate expressions in TB clearly demonstrated that each transferase indeed improves excretion based on extracellular curcumin fraction. Comparisons against FCS and CUS alone revealed that BbGT co-

expression most significantly improves extracellular curcumin fraction, improving the mean extracellular fraction from $31.0 \pm 1.8\%$ to $46.1 \pm 1.0\%$ ($p = 0.0025$), corresponding to an overall 48.7% improvement in curcumin excretion (percent change). The use of UGT and HoST also significantly improved excretion, yielding extracellular curcumin fractions of $40.2 \pm 2.1\%$ and $40.5 \pm 5.7\%$, respectively (Fig. 4.11).

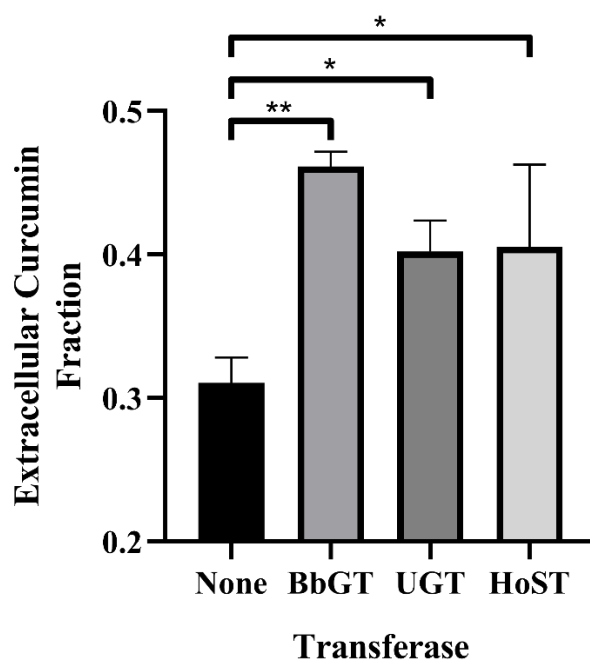


Figure 4.11: Fraction of total curcumin yield obtained from the cell-free culture medium (“extracellular fraction”) grouped by the transferase co-expressed with curcumin biosynthetic enzymes.

We were interested in knowing whether curcumin glycosides and curcumin sulfate existed predominantly in the extracellular fraction, consistent with our theory that glycosylation and sulfation can promote excretion from the cell. However, when expressed in TB with glycerol as a carbon source, very little glycosidic and sulfated products were detected, complicating the analysis. To attempt to extend induced expression time, we attempted expression in LB with the addition of ferulic acid 5 hours after induction by the addition of 0.1 mM IPTG and the delayed addition of glucose 18 hours after the addition of IPTG. These measures were implemented to attempt to postpone the deactivation of the lac operon contained in our expression constructs. We

were able to see marked improvements in curcumin glycoside and sulfated product peak areas, indicating that the delayed addition of glucose can boost the production of curcumin glucoside, curcumin glucuronide, and curcumin sulfate. We next compared the peak area data for each glycoside, glucuronide, and sulfated product from the LB expression experiment to determine the predominant location of each of the products. These data are presented in Table 4.5.

Table 4.5: Curcumin glycoside and sulfate product peak areas when expressed in LB with delayed addition of glucose.

Transferase	CFB Peak Area (mAU*s)	CWB Peak Area (mAU*s)	Extracellular Fraction
BbGT	76.9 ± 61.1	79.2 ± 58.5	49.30%
UGT	568.4 ± 118.5	412.2 ± 144.5	58.00%
HoST	12.7	9.4	57.50%

To better visualize the effect of transferase co-expression on curcumin excretion, we analyzed the location of curcumin, curcumin- x (where x represents glucoside, glucuronide, or sulfate), and “total curcumin” (the sum of curcumin and curcumin- x) for each expression system. Then, using the average peak areas for each treatment group, we calculated the mean extracellular

fraction as a ratio of the average CFB peak area over the average CWB peak area and plotted these as stacked columns for each curcumin, curcumin-*x*, and total curcumin (**Fig. 4.12**).

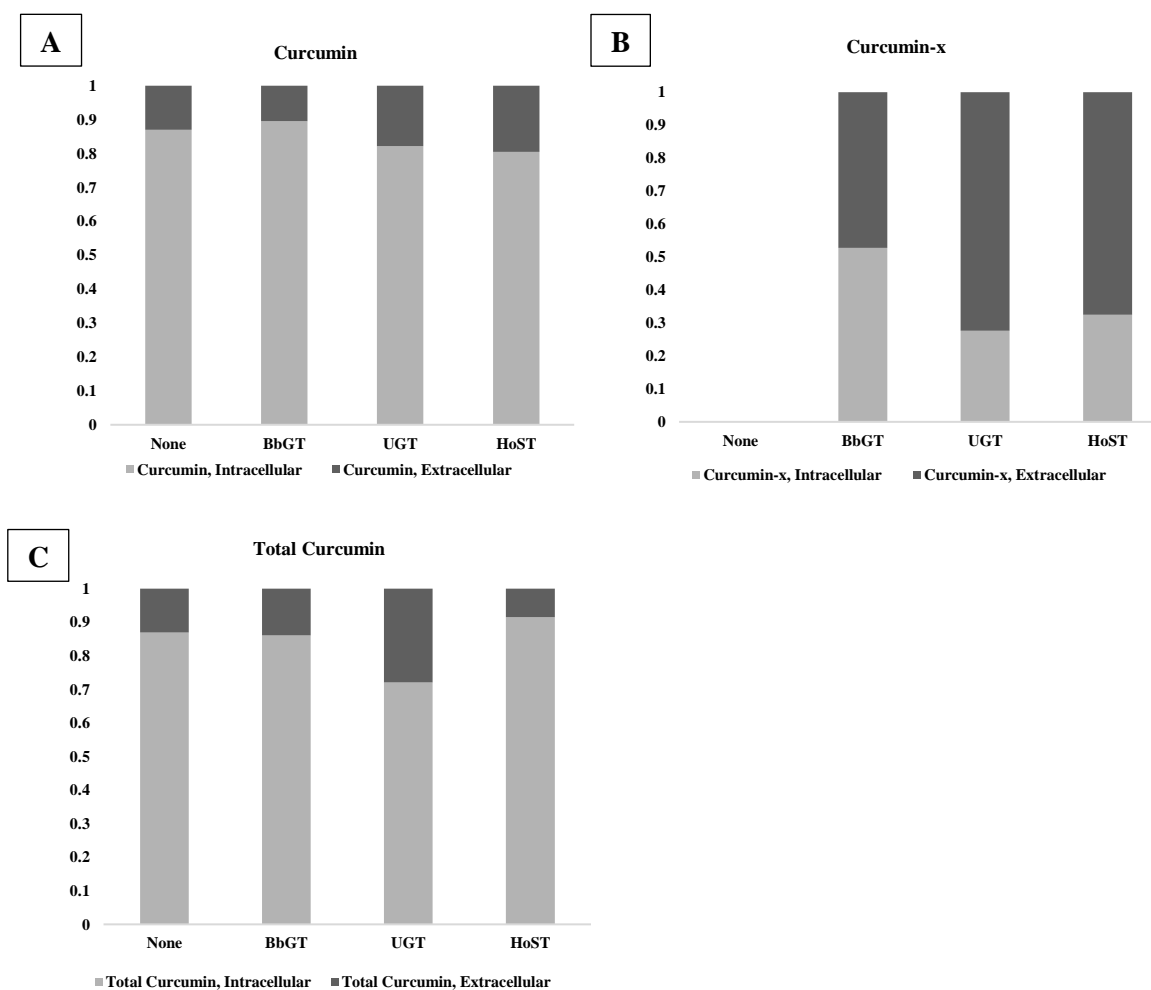


Figure 4.12: Visual representation of curcumin excretion based on transferase co-expression. (A) Curcumin extracellular fractions stacked on intracellular fractions; (B) Modified curcumin products (“curcumin-*x*”) extracellular fractions stacked on intracellular fractions; (C) Total curcumin extracellular fractions stacked on intracellular fractions.

This analysis demonstrated visually that the curcumin-*x* products indeed existed predominantly in the extracellular culture medium except for curcumin glucoside, which existed approximately half as an intracellular metabolite and half as an extracellular metabolite. Overall, the expression of UGT had the strongest impact on total curcumin excretion under the LB expression conditions.

4.8 Effect of Transferase Co-Expression on Total Curcumin Yield

Though the effect of curcumin excretion was well established for each transferase, the overall impact on yield was also investigated using the same TB expression system data obtained in section 4.7. Using the CWB titer as the “total curcumin” yield in the system with comparisons to FCS+CUS as the control, it was shown that curcumin yield was decreased in the case of each transferase treatment group (**Fig. 4.13**).

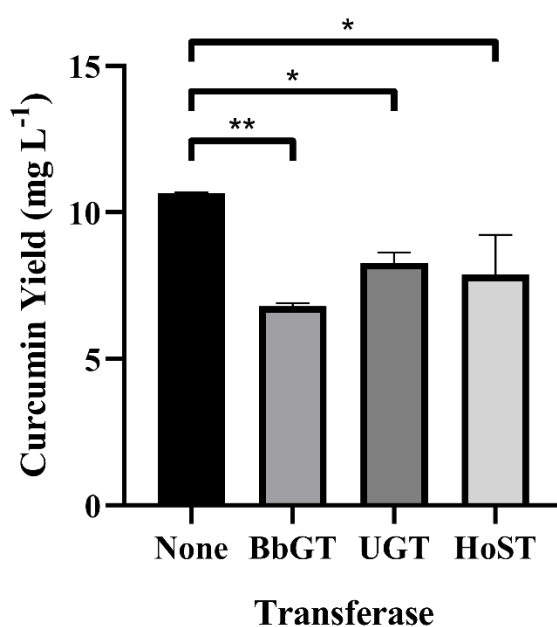


Figure 4.13: Total curcumin yield in mg L⁻¹ for each transferase treatment group.

The co-expression of BbGT with the curcumin biosynthetic enzymes had the strongest negative impact on curcumin production, while UGT and HoST had similar negative effects on curcumin production. Likely, this phenomenon can be explained in part by increased metabolic burden imposed on the cells by the co-expression of an additional enzyme. However, our group previously reported that UGT could accept ferulic acid as a substrate for the formation of ferulic acid-4-O- β -D-glucuronide.⁷⁸ This understanding gave rise to an alternative hypothesis that some ferulic acid was being glycosylated or sulfated prior to entering the curcumin biosynthetic

pathway, which may have sterically restricted its entry into the FCS and/or CUS catalytic domains, thereby reducing the formation of curcumin (**Fig. 4.14**).

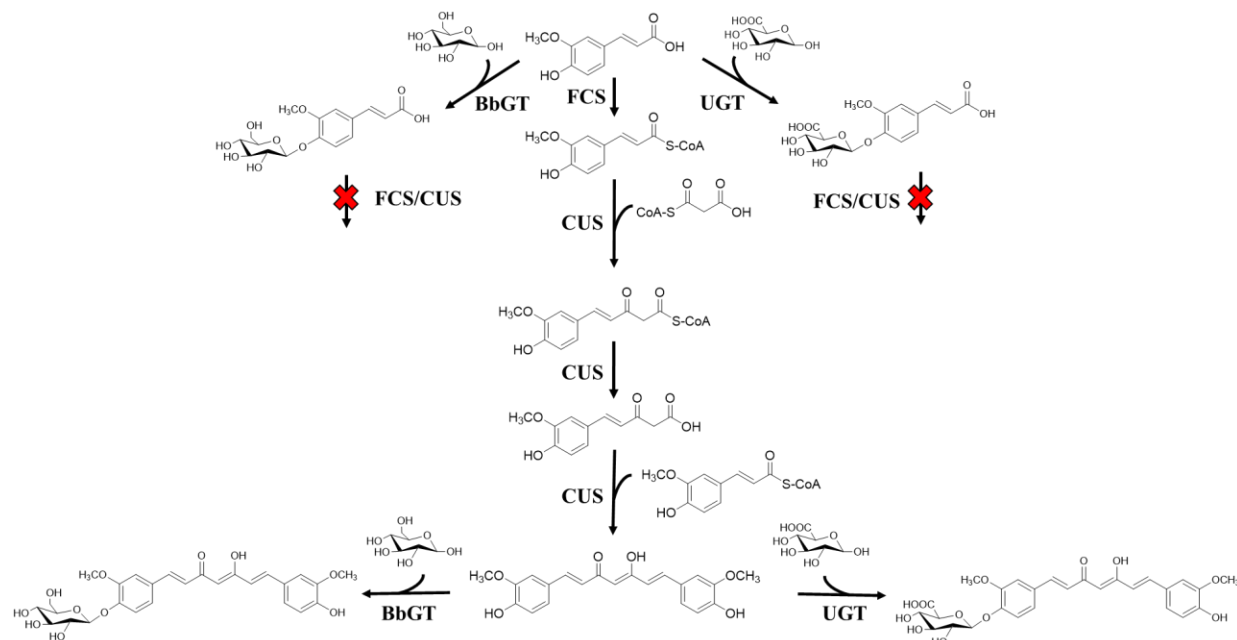


Figure 4.14: Proposed glycosylation pathways involved in FCS+CUS+BbGT and FCS+CUS+UGT co-expression systems. We hypothesize that glycosylation of ferulic acid preceding the curcumin biosynthetic steps reduces the formation of curcumin and its derivatives.

Therefore, we revisited our HPLC data collected for BbGT, UGT, and HoST co-expression systems, this time using a 300 nm wavelength to scan for ferulic acid and ferulic acid derivatives. We stacked the resulting HPLC chromatograms obtained from each transferase treatment group and compared them against the control (FCS+CUS). Indeed, the formation of ferulic acid derivatives were detected that did not exist in the control for BbGT- and UGT-containing samples. However, HoST showed no apparent activity toward ferulic acid (**Fig. 4.15**). ESI-MS data for the ferulic acid derivatives has yet to be collected, which is an important future step for validating the hypothesis.

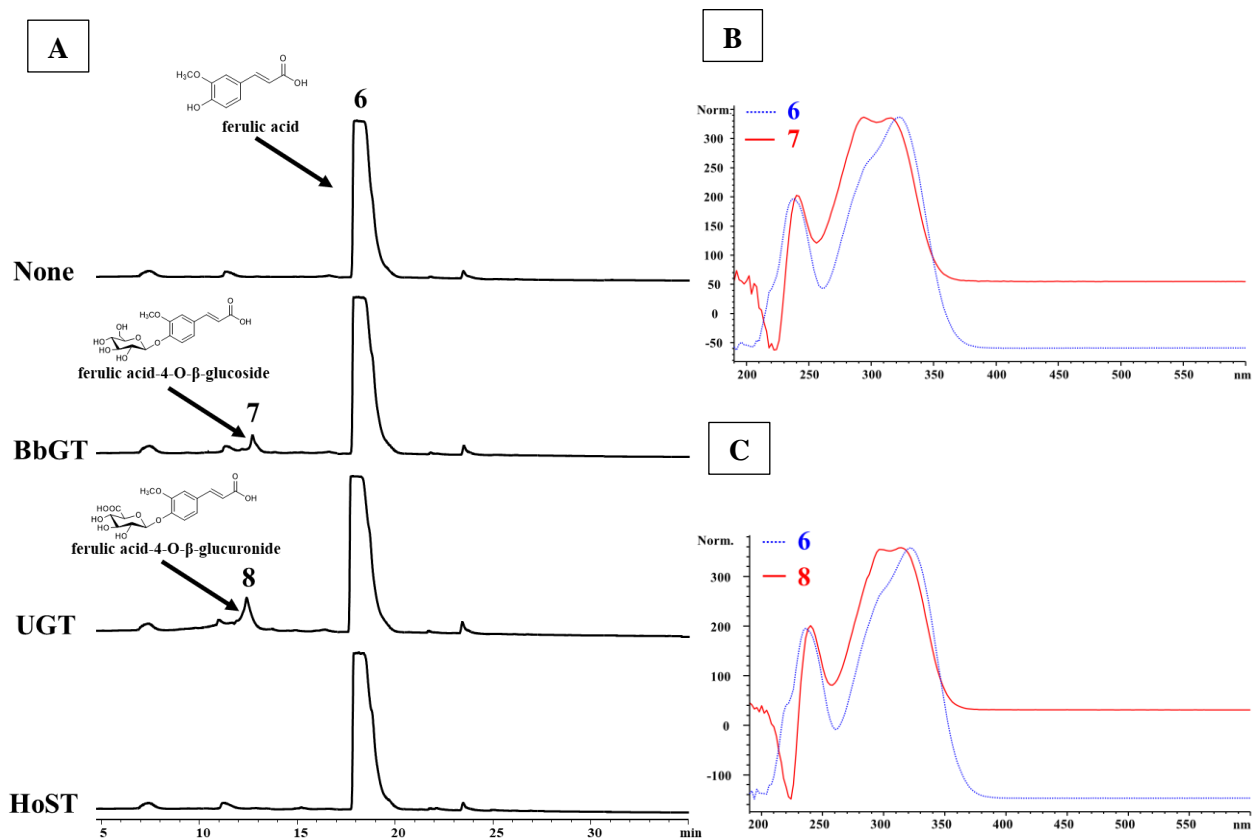


Figure 4.15: Glycosylation of ferulic acid (6) may be a factor for reducing curcumin productivity. (A) Stacked chromatograms of each transferase treatment group with FCS+CUS serving as a negative control (“None”). The likely formation of ferulic acid-4-O-β-glucoside (7) and ferulic acid-4-O-β-glucuronide (8) are shown with reduced retention times, corresponding to higher water solubility; (B) Overlaid UV-Vis spectra of peaks 6 and 7 suggest that the product is derived from ferulic acid; (C) Overlaid UV-Vis spectra of peaks 6 and 8 suggest that the product is derived from ferulic acid.

CHAPTER V

Conclusions

Herein, several upstream biological engineering methods have been investigated to improve the heterologous production of curcumin in *E. coli*. Each of the reported methods represent an improvement in curcumin yield, expanding the toolbox for future researchers and industry professionals, thereby improving access to this pharmaceutically relevant compound.

First, we reported the discovery of an efficient FCS that can improve the feruloyl-CoA precursor metabolite pool. Isolation and *in vitro* analysis of these enzymes revealed that the FCS has higher catalytic efficiency but lower binding affinity for the ferulic acid substrate, for a net improvement in k_{cat}/K_m . These findings suggest that the use of 4507FCS can improve curcumin production under saturation conditions, but that At4CL1 may be the enzyme of choice if lower concentrations of ferulic acid are utilized. Furthermore, we demonstrated that though FCS exhibits higher k_{cat}/K_m , the expression levels remain low relative to At4CL1. Further work should seek to improve 4507FCS expression to build its commercial relevance in the curcumin biosynthetic pathway. Various methods may be employed to improve 4507FCS expression, including codon optimization and optimization studies on 4507FCS induction parameters.

The use of FCSs from various hosts paves the way for future researchers to continue FCS screening to potentially identify other efficient FCSs that can be used not only to achieve curcumin biosynthesis, but also for the biosynthesis of other compounds that rely on feruloyl-CoA as a precursor, such as vanillin,⁸⁶ coumarins,⁸⁷ and lignans.⁸⁸ This study focused on a limited number of FCSs, thus the possibility of discovering another with further improved activity remains a possibility.

Direct comparisons on the *in vitro* enzymatic activities of At4CL1 and 4507FCS elucidated the mechanism by which 4507FCS improves curcumin biosynthesis, specifically by enhanced catalytic efficiency. These findings may encourage structural biologists to analyze the key residues involved in enhancing catalytic efficiency for feruloyl-CoA formation, which may allow for enzyme engineering and the development of an “ideal” FCS in the coming years.

The importance of DCS in the biosynthetic pathway has been clearly demonstrated in this thesis, therefore giving clear confirmation that the rate-limiting step in the curcumin biosynthetic pathway is the formation of feruloyl-diketide-CoA from feruloyl-CoA and malonyl-CoA. The marked improvement in curcumin biosynthesis in DCS-containing co-expression systems suggests that the polyketide synthetic domain of CUS responsible for condensing malonyl-CoA with feruloyl-CoA to form feruloyl-diketide CoA may not be as efficient as that of DCS. However, the CURS1 appears to have improved condensation activity over CUS for the formation of β -ketoacid and curcumin from their precursors, as demonstrated by the maximized yield from the DCS/CURS1 co-expression system. Together, these findings may encourage protein engineers to develop a fusion protein that brings the catalytic domains of DCS and CURS1 in closer proximity to test the effect on curcumin biosynthesis, which we hypothesize would have a positive impact on productivity. Furthermore, these findings demonstrate that the FCS-catalyzed reaction is not the limiting step in the curcumin biosynthetic pathway, and that more research effort should be placed on the condensation steps.

To our knowledge, the use of glycosylation and sulfation as reported in this thesis are the first reported mechanisms for exporting curcumin from the heterologous production host. Significant improvements in curcumin excretion using these modifications suggest that *E. coli* may take advantage of the same detoxification mechanisms observed in human metabolism. These

findings also represent the first time that BbGT, UGT, and HoST have successfully formed glycosylated or sulfated curcumin products in an *in vivo* system, since previous studies only reported on their activities towards curcumin *in vitro*. These methods form a basis for the eventual use of continuous fermentation systems, greatly reducing the cost of curcumin biosynthesis and increasing the benefits of its heterologous production over agricultural methods. Additionally, these findings provide a biosynthetic approach to produce more water soluble and bioavailable forms of curcumin, including curcumin glucoside, curcumin glucuronide, and curcumin sulfate, with direct applications for human health.

Though the efficiency of the overall curcumin production system was decreased when co-expressing a transferase, we hypothesize that this is in part the effect of increased metabolic burden, which may be readily circumvented by constructing a plasmid that encodes each of the needed proteins for curcumin production and glycosylation or sulfation. Additionally, the curcumin and modified curcumin yields may also be improved by constructing a plasmid carrying the *fcs*, *dcs* and *curS1* genes for co-expression with a transferase. In the case of glycosylation, we also hypothesize that the reduced curcumin production may be the result of substrate glycosylation prior to entering the curcumin biosynthetic pathway. This issue is not easily resolved but could be the subject of future enzyme engineering studies. For example, the catalytic domains of FCS and CUS could be engineered to open wide enough to accept a glycosylated substrate if steric hindrance is in fact at play.

CHAPTER VI

Engineering Value and Future Work

6.1 Engineering Value

In this thesis, several engineering approaches have been employed to enhance the heterologous production of curcumin in *E. coli*. First, the characterization of several FCSs that may be used to replace 4CL creates a modular toolbox that may be used not only for the biosynthesis of curcumin, but also for other valuable bioproducts that require feruloyl-CoA as a precursor, such as vanillin, lignans, and coumarins. We also elucidated the exact mechanism and conditions under which 4507FCS improves curcumin biosynthesis over At4CL1, which provides valuable information for the development of biochemical engineering processes, specifically the tuning of substrate concentrations to optimize system efficacy.

Furthermore, this work clearly demonstrates the limiting step in the curcumin biosynthetic pathway, which is the condensation step catalyzed by DCS, which provides a target for future enzyme engineering and metabolic engineering strategies that may be used to efficiently optimize curcumin biosynthesis. This limiting step can be viewed as an engineering constraint that ought to be the focus of future research to expand the possibilities for further yield improvements.

Finally, this thesis provides a method for enzymatically modifying curcumin to improve its water solubility and allow for improved excretion from the cell. These advances provide biochemical engineers with a tool for the development of continuous fermentation systems that can greatly reduce the energy, time, and complexity of curcumin downstream processing by eliminating the need for cell disruption.

6.2 Future Work

6.2.1 Individual Enzyme Expression Optimization

Little work was performed in this thesis to improve the expression levels of the individual enzymes participating in the curcumin biosynthetic pathway. Future work should focus on maximizing the expression of each individual protein in the pathway, then developing a method that allows for combinatorial curcumin biosynthesis using the method that most appropriately supports high expression for the enzyme combination selected. Special focus should be placed on improving 4507FCS expression in *E. coli*. Potential methods may include codon optimization and optimization of induction parameters to harness the full potential of this enzyme.

6.2.2 Improving Curcumin Glycoside and Curcumin Sulfate Production

We hypothesize that curcumin glycoside and sulfate production may be greatly enhanced if DCS and CURS1 are used as the condensing enzymes in place of CUS. In this thesis, we only explored the use of CUS with the transferase enzymes in the interest of time and minimizing metabolic burden, but future work could consider the use of a single construct encoding each of the biosynthetic enzymes needed to achieve simultaneous curcumin production and glycosylation/sulfation (i.e. FCS, DCS, CURS1, and BbGT on one or two constructs instead of each being encoded on individual constructs).

Methods should also be implemented to limit the glycosylation of ferulic acid substrate prior to entering the curcumin biosynthetic pathway. For example, one synthetic biological approach may employ the use of constitutive promoters for the curcumin biosynthetic genes together with the use of an inducible promoter for the transferase gene. In this way, the curcumin

metabolic pool could be built up prior to the induction of the transferase gene to improve the efficiency of the glycosylation pathways.

6.2.3 Structural Studies and Enzyme Engineering

Much structural information about the key catalytic residues of the enzymes involved in curcumin biosynthesis is left unexplored in this work. Future studies could compare the catalytic regions of At4CL1 and 4507FCS for better understanding the key differences that allow for upregulating the formation of feruloyl-CoA.

Additionally, as we postulated in this thesis, many enzyme engineering applications need continued study, especially the effect of DCS-CURS1 proximity on productivity. A fusion of these two enzymes is theorized to improve yield by bringing their catalytic domains closer together to reduce the diffusion limitations of curcumin metabolic intermediates.

6.2.4 Biochemical Process Development and Optimization

To improve the industrial application of the work performed in this thesis, curcumin production should be performed in a bioreactor. An appropriate operating mode should be selected for optimizing curcumin production (batch, fill and draw, continuous, etc.), then different retention times, substrate concentrations, oxygenation methods, and mixing speeds should be evaluated. Continuous fermentation systems should be the first target for curcumin production to improve product consistency, reduce operating costs, and minimize downstream processing. Conditions should also be optimized to produce curcumin glucoside, curcumin glucuronide, and curcumin sulfate to improve access to more bioavailable forms of curcumin.

Additionally, bioreactor studies could consider reducing operating costs by using cheaper carbon sources, such as crude glycerol arising from biodiesel production to reduce the overall costs associated with curcumin biosynthesis. Cheaper nitrogen sources may also be tested. For example, algae has been successfully used in several studies for the denitrification of wastewaters,⁸⁹⁻⁹¹ yielding nitrogen-rich algae whose lysate could be fed as a nitrogen source to engineered *E. coli* for curcumin production.

REFERENCES

1. Gokulan, K., Khare, S. & Cerniglia, C. Metabolic Pathways | Production of secondary metabolites of bacteria. *Encyclopedia of Food Microbiology (Second Edition)* (eds. Batt, C. A. & Tortorello, M. L.) 561–569 (Academic Press, 2014). doi:10.1016/B978-0-12-384730-0.00203-2.
2. Sun, L., Zeng, J., Zhang, S., Gladwin, T. & Zhan, J. Effects of exogenous nutrients on polyketide biosynthesis in *Escherichia coli*. *Appl. Microbiol. Biotechnol.* **99**, 693–701 (2015).
3. Yu, D., Xu, F., Zeng, J. & Zhan, J. Type III polyketide synthases in natural product biosynthesis. *IUBMB Life* **64**, 285–295 (2012).
4. Hatcher, H., Planalp, R., Cho, J., Torti, F. M. & Torti, S. V. Curcumin: From ancient medicine to current clinical trials. *Cell. Mol. Life Sci. CMLS* **65**, 1631–1652 (2008).
5. Zaman, M. S. *et al.* Curcumin nanoformulation for cervical cancer treatment. *Sci. Rep.* **6**, 20051 (2016).
6. Menon, V. P. & Sudheer, A. R. Antioxidant and anti-inflammatory properties of curcumin. *The Molecular Targets and Therapeutic Uses of Curcumin in Health and Disease* (eds. Aggarwal, B. B., Surh, Y.-J. & Shishodia, S.) 105–125 (Springer US, 2007). doi:10.1007/978-0-387-46401-5_3.
7. Weisberg, S., Leibel, R. & Tortorello, D. V. Proteasome inhibitors, including curcumin, improve pancreatic β -cell function and insulin sensitivity in diabetic mice. *Nutr. Diabetes* **6**, e205–e205 (2016).
8. Shen, L., Liu, C.-C., An, C.-Y. & Ji, H.-F. How does curcumin work with poor bioavailability? Clues from experimental and theoretical studies. *Sci. Rep.* **6**, 20872 (2016).
9. Kunnumakkara, A. B. *et al.* Curcumin, the golden nutraceutical: multitargeting for multiple chronic diseases. *Br. J. Pharmacol.* **174**, 1325–1348 (2017).
10. Wong, K. E. *et al.* Curcumin nanoformulations for colorectal cancer: A Review. *Front. Pharmacol.* **10**, (2019).

11. Mahjoob, M. & Stochaj, U. Curcumin nanoformulations to combat aging-related diseases. *Ageing Res. Rev.* **69**, 101364 (2021).
12. Pawar, K. S. *et al.* Oral curcumin with piperine as adjuvant therapy for the treatment of COVID-19: A randomized clinical trial. *Front. Pharmacol.* **12**, (2021).
13. Praditya, D. *et al.* Anti-infective properties of the golden spice curcumin. *Front. Microbiol.* **10**, (2019).
14. von Rhein, C. *et al.* Curcumin and *Boswellia serrata* gum resin extract inhibit chikungunya and vesicular stomatitis virus infections in vitro. *Antiviral Res.* **125**, 51–57 (2016).
15. Chen, T.-Y. *et al.* Inhibition of enveloped viruses infectivity by curcumin. *PLOS ONE* **8**, e62482 (2013).
16. Anggakusuma *et al.* Turmeric curcumin inhibits entry of all hepatitis C virus genotypes into human liver cells. *Gut* **63**, 1137–1149 (2014).
17. Ou, J.-L. *et al.* Structure–activity relationship analysis of curcumin analogues on anti-influenza virus activity. *FEBS J.* **280**, 5829–5840 (2013).
18. Yang, M. *et al.* Curcumin shows antiviral properties against norovirus. *Molecules* **21**, 1401 (2016).
19. Yang, X. X., Li, C. M. & Huang, C. Z. Curcumin modified silver nanoparticles for highly efficient inhibition of respiratory syncytial virus infection. *Nanoscale* **8**, 3040–3048 (2016).
20. Mounce, B. C., Cesaro, T., Carrau, L., Vallet, T. & Vignuzzi, M. Curcumin inhibits Zika and chikungunya virus infection by inhibiting cell binding. *Antiviral Res.* **142**, 148–157 (2017).
21. Padilla-S, L., Rodríguez, A., Gonzales, M. M., Gallego-G, J. C. & Castaño-O, J. C. Inhibitory effects of curcumin on dengue virus type 2-infected cells in vitro. *Arch. Virol.* **159**, 573–579 (2014).
22. Kim, H. J. *et al.* Antiviral effect of *Curcuma longa* Linn extract against hepatitis B virus replication. *J. Ethnopharmacol.* **124**, 189–196 (2009).
23. Yang, X. X., Li, C. M., Li, Y. F., Wang, J. & Huang, C. Z. Synergistic antiviral effect of curcumin functionalized graphene oxide against respiratory syncytial virus infection. *Nanoscale* **9**, 16086–16092 (2017).

24. Narayanan, A. *et al.* Curcumin inhibits rift valley fever virus replication in human cells*. *J. Biol. Chem.* **287**, 33198–33214 (2012).
25. Mouler Rechtman, M. *et al.* Curcumin inhibits hepatitis B virus via down-regulation of the metabolic coactivator PGC-1 α . *FEBS Lett.* **584**, 2485–2490 (2010).
26. Wei, Z.-Q. *et al.* Curcumin inhibits hepatitis B virus infection by down-regulating cccDNA-bound histone acetylation. *World J. Gastroenterol.* **23**, 6252–6260 (2017).
27. Sui, Z., Salto, R., Li, J., Craik, C. & Ortiz de Montellano, P. R. Inhibition of the HIV-1 and HIV-2 proteases by curcumin and curcumin boron complexes. *Bioorg. Med. Chem.* **1**, 415–422 (1993).
28. Mazumder, A., Raghavan, K., Weinstein, J., Kohn, K. W. & Pommier, Y. Inhibition of human immunodeficiency virus type-1 integrase by curcumin. *Biochem. Pharmacol.* **49**, 1165–1170 (1995).
29. Ali, A. & Banerjea, A. C. Curcumin inhibits HIV-1 by promoting Tat protein degradation. *Sci. Rep.* **6**, 27539 (2016).
30. Mishra, A. *et al.* Curcumin modulates cellular AP-1, NF-kB, and HPV16 E6 proteins in oral cancer. *eCancer.* **9**:525 (2015).
31. Kutluay, S. B., Doroghazi, J., Roemer, M. E. & Triezenberg, S. J. Curcumin inhibits herpes simplex virus immediate-early gene expression by a mechanism independent of p300/CBP histone acetyltransferase activity. *Virology* **373**, 239–247 (2008).
32. Bhawana, Basniwal, R. K., Buttar, H. S., Jain, V. K. & Jain, N. Curcumin nanoparticles: preparation, characterization, and antimicrobial study. *J. Agric. Food Chem.* **59**, 2056–2061 (2011).
33. Tajbakhsh, S. *et al.* Antibacterial activity of indium curcumin and indium diacetylcurcumin. *Afr. J. Biotechnol.* **7**, (2008).
34. Betts, J. W., Sharili, A. S., La Ragione, R. M. & Wareham, D. W. In vitro antibacterial activity of curcumin–polymyxin B combinations against multidrug-resistant bacteria associated with traumatic wound infections. *J. Nat. Prod.* **79**, 1702–1706 (2016).

35. de Oliveira, E. F., Tosati, J. V., Tikekar, R. V., Monteiro, A. R. & Nitin, N. Antimicrobial activity of curcumin in combination with light against *Escherichia coli* O157:H7 and *Listeria innocua*: Applications for fresh produce sanitation. *Postharvest Biol. Technol.* **137**, 86–94 (2018).
36. Tønnesen, H. H., de Vries, H., Karlsen, J. & Van Henegouwen, G. B. Studies on curcumin and curcuminoids ix: investigation of the photobiological activity of curcumin using bacterial indicator systems. *J. Pharm. Sci.* **76**, 371–373 (1987).
37. Jaiswal, S. & Mishra, P. Antimicrobial and antibiofilm activity of curcumin-silver nanoparticles with improved stability and selective toxicity to bacteria over mammalian cells. *Med. Microbiol. Immunol. (Berl.)* **207**, 39–53 (2018).
38. Song, J., Choi, B., Jin, E.-J., Yoon, Y. & Choi, K.-H. Curcumin suppresses *Streptococcus mutans* adherence to human tooth surfaces and extracellular matrix proteins. *Eur. J. Clin. Microbiol. Infect. Dis.* **31**, 1347–1352 (2012).
39. Park, B.-S. *et al.* *Curcuma longa* L. constituents inhibit Sortase A and *Staphylococcus aureus* cell adhesion to fibronectin. *J. Agric. Food Chem.* **53**, 9005–9009 (2005).
40. Lee, W. & Lee, D. G. An antifungal mechanism of curcumin lies in membrane-targeted action within *Candida albicans*. *IUBMB Life* **66**, 780–785 (2014).
41. Wang, T. & Chen, J. Effects of curcumin on vessel formation: Insight into the pro- and antiangiogenesis of curcumin. *Evid.-Based Complement. Altern. Med. ECAM* **2019**, 1390795 (2019).
42. Bhandarkar, S. S. & Arbiser, J. L. Curcumin as an inhibitor of angiogenesis. in *The Molecular Targets and Therapeutic Uses of Curcumin in Health and Disease* (eds. Aggarwal, B. B., Surh, Y.-J. & Shishodia, S.) 185–195 (Springer US, 2007). doi:10.1007/978-0-387-46401-5_7.
43. Sidhu, G. S. *et al.* Enhancement of wound healing by curcumin in animals. *Wound Repair Regen.* **6**, 167–177 (1998).
44. Krausz, A. E. *et al.* Curcumin-encapsulated nanoparticles as innovative antimicrobial and wound healing agent. *Nanomedicine Nanotechnol. Biol. Med.* **11**, 195–206 (2015).

45. Partoazar, A. *et al.* Ethosomal curcumin promoted wound healing and reduced bacterial flora in second degree burn in rat. *Drug Res.* **66**, 660–665 (2016).
46. Carvalho Ferreira, L. *et al.* Effect of curcumin on pro-angiogenic factors in the xenograft model of breast cancer. *Anti-Cancer Agents Med. Chem.- Anti-Cancer Agents* **15**, 1285–1296 (2015).
47. Scazzocchio, B., Minghetti, L. & D'Archivio, M. Interaction between gut microbiota and curcumin: A new key of understanding for the health effects of curcumin. *Nutrients* **12**, 2499 (2020).
48. Zhai, S. S. *et al.* Protective effect of curcumin on ochratoxin A–induced liver oxidative injury in duck is mediated by modulating lipid metabolism and the intestinal microbiota. *Poult. Sci.* **99**, 1124–1134 (2020).
49. Geurts, L. *et al.* Altered gut microbiota and endocannabinoid system tone in obese and diabetic leptin-resistant mice: impact on apelin regulation in adipose tissue. *Front. Microbiol.* **2**, (2011).
50. Zhang, Z. *et al.* Effect of curcumin on the diversity of gut microbiota in ovariectomized rats. *Nutrients* **9**, 1146 (2017).
51. Liu, Z.-J. *et al.* Curcumin attenuates beta-amyloid-induced neuroinflammation via activation of peroxisome proliferator-activated receptor-gamma function in a rat model of Alzheimer's disease. *Front. Pharmacol.* **7**, (2016).
52. Rashmi, R., Santhosh Kumar, T. r. & Karunagaran, D. Human colon cancer cells differ in their sensitivity to curcumin-induced apoptosis and heat shock protects them by inhibiting the release of apoptosis-inducing factor and caspases. *FEBS Lett.* **538**, 19–24 (2003).
53. Rodrigues, J. L., Prather, K. L. J., Kluskens, L. D. & Rodrigues, L. R. Heterologous production of curcuminoids. *Microbiol. Mol. Biol. Rev.* **79**, 39–60.
54. Zhang, R., Li, S., Zhu, Z. & He, J. Recent advances in valorization of Chaenomeles fruit: A review of botanical profile, phytochemistry, advanced extraction technologies and bioactivities. *Trends Food Sci. Technol.* **91**, 467–482 (2019).
55. Jiang, T., Ghosh, R. & Charcosset, C. Extraction, purification and applications of curcumin from plant materials: A comprehensive review. *Trends Food Sci. Technol.* **112**, 419–430 (2021).

56. Couto, M. R., Rodrigues, J. L. & Rodrigues, L. R. Optimization of fermentation conditions for the production of curcumin by engineered *Escherichia coli*. *J. R. Soc. Interface* **14**, 20170470 (2017).
57. Machado, D., Rodrigues, L. R. & Rocha, I. A kinetic model for curcumin production in *Escherichia coli*. *Biosystems* **125**, 16–21 (2014).
58. Wu, J. *et al.* Metabolic Engineering for Improved Curcumin Biosynthesis in *Escherichia coli*. *J. Agric. Food Chem.* **68**, 10772–10779 (2020).
59. Rodrigues, J. L. L. C., Couto, M. R. & Rodrigues, L. R. Heterologous production of plant natural polyphenolic compounds in *Escherichia coli*. (2017).
60. Machado, C. D., Rodrigues, L. R. & Rocha, I. Design of a biosynthetic pathway for curcumin production in *Escherichia coli*. (2012).
61. Kan, E. *et al.* Production of the plant polyketide curcumin in *Aspergillus oryzae*: strengthening malonyl-CoA supply for yield improvement. *Biosci. Biotechnol. Biochem.* **83**, 1372–1381 (2019).
62. Rainha, J., Rodrigues, J. L., Faria, C. & Rodrigues, L. R. Curcumin biosynthesis from ferulic acid by engineered *Saccharomyces cerevisiae*. *Biotechnol. J.* **17**, 2100400 (2022).
63. Singh, S., Pandey, P., Akhtar, Md. Q., Negi, A. S. & Banerjee, S. A new synthetic biology approach for the production of curcumin and its glucoside in *Atropa belladonna* hairy roots. *J. Biotechnol.* **328**, 23–33 (2021).
64. Rodrigues, J. L., Gomes, D. & Rodrigues, L. R. A combinatorial approach to optimize the production of curcuminoids from tyrosine in *Escherichia coli*. *Front. Bioeng. Biotechnol.* **8**, 59 (2020).
65. Rodrigues, J. L., Araújo, R. G., Prather, K. L. J., Kluskens, L. D. & Rodrigues, L. R. Production of curcuminoids from tyrosine by a metabolically engineered *Escherichia coli* using caffeic acid as an intermediate. *Biotechnol. J.* **10**, 599–609 (2015).
66. Wang, S. *et al.* Metabolic engineering of *Escherichia coli* for the biosynthesis of various phenylpropanoid derivatives. *Metab. Eng.* **29**, 153–159 (2015).
67. Horinouchi, S. Combinatorial biosynthesis of non-bacterial and unnatural flavonoids, stilbenoids and curcuminoids by microorganisms. *J. Antibiot. (Tokyo)* **61**, 709–728 (2008).

68. Amalraj, A., Pius, A., Gopi, S. & Gopi, S. Biological activities of curcuminoids, other biomolecules from turmeric and their derivatives – A review. *J. Tradit. Complement. Med.* **7**, 205–233 (2017).
69. Priyadarsini, K. I. Photophysics, photochemistry and photobiology of curcumin: Studies from organic solutions, bio-mimetics and living cells. *J. Photochem. Photobiol. C Photochem. Rev.* **10**, 81–95 (2009).
70. Katsuyama, Y., Matsuzawa, M., Funa, N. & Horinouchi, S. 2008. Production of curcuminoids by *Escherichia coli* carrying an artificial biosynthesis pathway. *Microbiology* **154**, 2620–2628 (2008).
71. Tyagi, P., Singh, M., Kumari, H., Kumari, A. & Mukhopadhyay, K. Bactericidal activity of curcumin I is associated with damaging of bacterial membrane. *PLoS ONE* **10**, e0121313 (2015).
72. Yun, D. G. & Lee, D. G. Antibacterial activity of curcumin via apoptosis-like response in *Escherichia coli*. *Appl. Microbiol. Biotechnol.* **100**, 5505–5514 (2016).
73. Rahman, A., Linton, E., Hatch, A. D., Sims, R. C. & Miller, C. D. Secretion of polyhydroxybutyrate in *Escherichia coli* using a synthetic biological engineering approach. *J. Biol. Eng.* **7**, 24 (2013).
74. Guidoboni, G. E. Continuous fermentation systems for alcohol production. *Enzyme Microb. Technol.* **6**, 194–200 (1984).
75. Desmet, T. *et al.* Enzymatic glycosylation of small molecules: Challenging substrates require tailored catalysts. *Chem. – Eur. J.* **18**, 10786–10801 (2012).
76. Zeng, J., Yang, N., Li, X.-M., Shami, P. J. & Zhan, J. 4'-O-Methylglycosylation of curcumin by *Beauveria bassiana*. *Nat. Prod. Commun.* **5**, 1934578X1000500119 (2010).
77. Ren, J. *et al.* A highly versatile fungal glucosyltransferase for specific production of quercetin-7-O- β -d-glucoside and quercetin-3-O- β -d-glucoside in different hosts. *Appl. Microbiol. Biotechnol.* **106**, 227–245 (2022).
78. Ren, J., Barton, C. D., Sorenson, K. E. & Zhan, J. Identification of a novel glucuronyltransferase from *Streptomyces chromofuscus* ATCC 49982 for natural product glucuronidation. *Appl. Microbiol. Biotechnol.* (2022) doi:10.1007/s00253-022-11789-2.

79. Stohs, S. J. *et al.* Highly bioavailable forms of curcumin and promising avenues for curcumin-based research and application: A review. *Molecules* **25**, 1397 (2020).
80. Jamil, Q. U. A., Jaerapong, N., Zehl, M., Jarukamjorn, K. & Jäger, W. Metabolism of curcumin in human breast cancer cells: Impact of sulfation on cytotoxicity. *Planta Med.* **83**, 1028–1034 (2017).
81. Sodr , V. *et al.* An alkaline active feruloyl-CoA synthetase from soil metagenome as a potential key enzyme for lignin valorization strategies. *PLOS ONE* **14**, e0212629 (2019).
82. Joyce, S. A. *et al.* Bacterial biosynthesis of a multipotent stilbene. *Angew. Chem. Int. Ed.* **47**, 1942–1945 (2008).
83. Mori, T. *et al.* Structural insight into the enzymatic formation of bacterial stilbene. *Cell Chem. Biol.* **23**, 1468–1479 (2016).
84. Carvalho, D. de M., Takeuchi, K. P., Geraldine, R. M., Moura, C. J. de & Torres, M. C. L. Production, solubility and antioxidant activity of curcumin nanosuspension. *Food Sci. Technol.* **35**, 115–119 (2015).
85. Ayuso-Fern ndez, I., Galm s, M. A., Bastida, A. & Garc a-Junceda, E. Aryl Sulfotransferase from *Haliangium ochraceum*: A versatile tool for the sulfation of small molecules. *ChemCatChem* **6**, 1059–1065 (2014).
86. Kundu, A. Vanillin biosynthetic pathways in plants. *Planta* **245**, 1069–1078 (2017).
87. Yang, S.-M., Shim, G. Y., Kim, B.-G. & Ahn, J.-H. Biological synthesis of coumarins in *Escherichia coli*. *Microb. Cell Factories* **14**, 65 (2015).
88. Yang, J., Wen, L., Jiang, Y. & Yang, B. Natural estrogen receptor modulators and their heterologous biosynthesis. *Trends Endocrinol. Metab.* **30**, 66–76 (2019).
89. Iman Shayan, S., Agblevor, F. A., Bertin, L. & Sims, R. C. Hydraulic retention time effects on wastewater nutrient removal and bioproduct production via rotating algal biofilm reactor. *Bioresour. Technol.* **211**, 527–533 (2016).

90. Hillman, K. M. & Sims, R. C. Struvite formation associated with the microalgae biofilm matrix of a rotating algal biofilm reactor (RABR) during nutrient removal from municipal wastewater. *Water Sci. Technol.* **81**, 644–655 (2020).
91. Wood, J. L., Takemoto, J. Y. & Sims, R. C. Rotating Algae Biofilm Reactor for management and valorization of produced wastewater. *Front. Energy Res.* **10**, (2022).

APPENDICES

Appendix A. Supplemental Spectral Data
for Confirmation of Various Curcuminoids

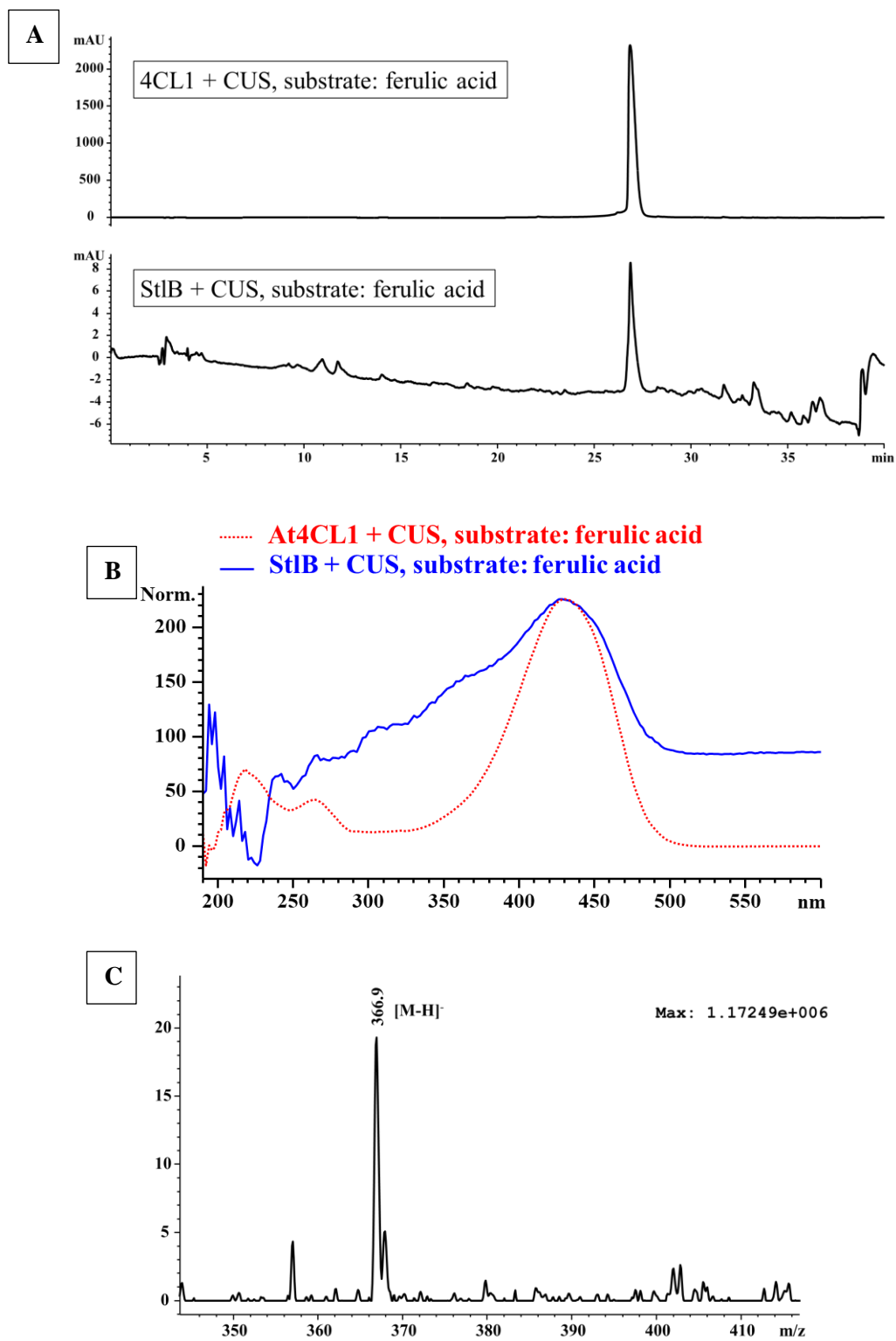


Figure A.1: Confirmation of curcumin formation by StlB with (A) retention time analysis, (B) UV-Vis spectral analysis and (C) ESI-MS spectral analysis

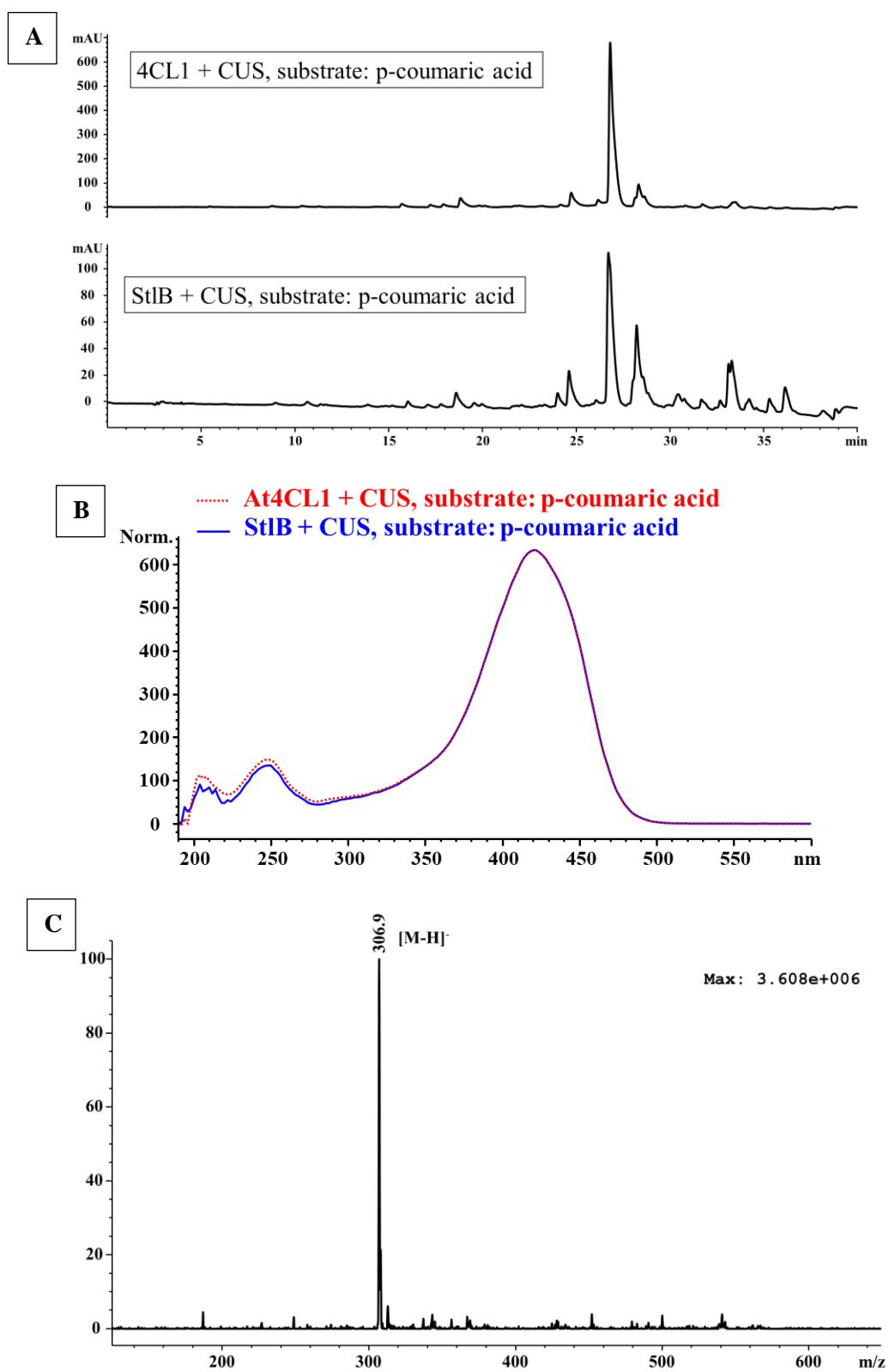


Figure A.2: Confirmation of bisdemethoxycurcumin formation by StlB with (A) retention time analysis, (B) UV-Vis spectral analysis and (C) ESI-MS spectral analysis

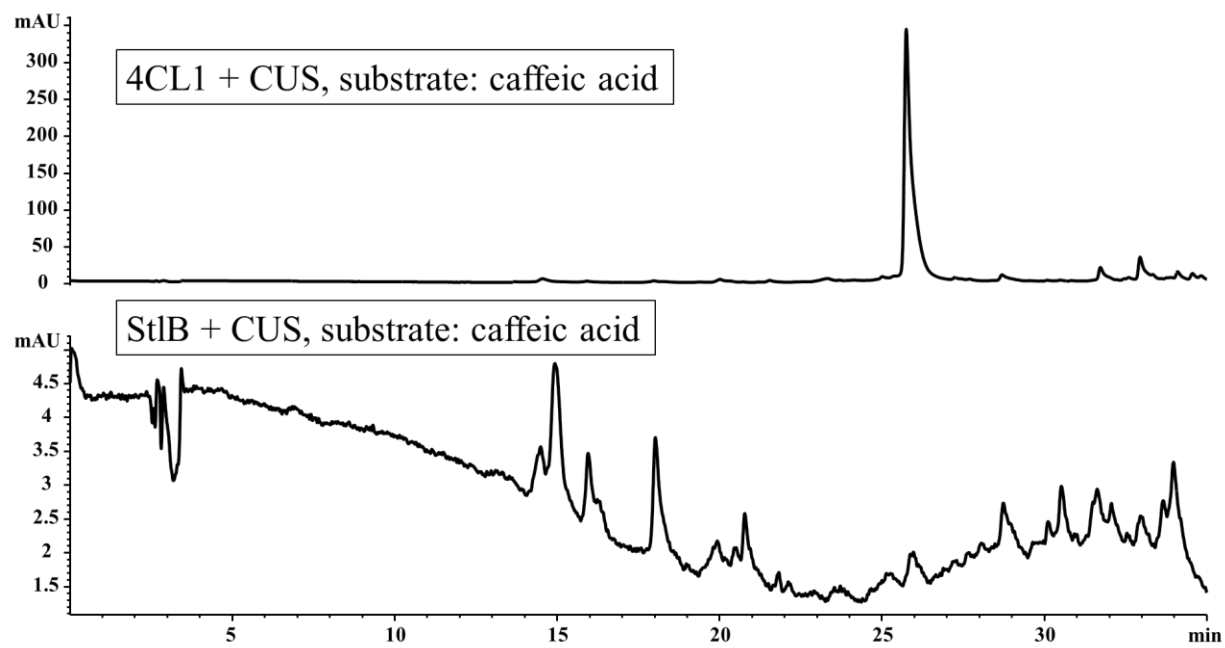


Figure A.3: No dicaffeoylmethane formation by StlB + CUS confirmed by retention time analysis shows that StlB cannot accept caffeic acid as a substrate

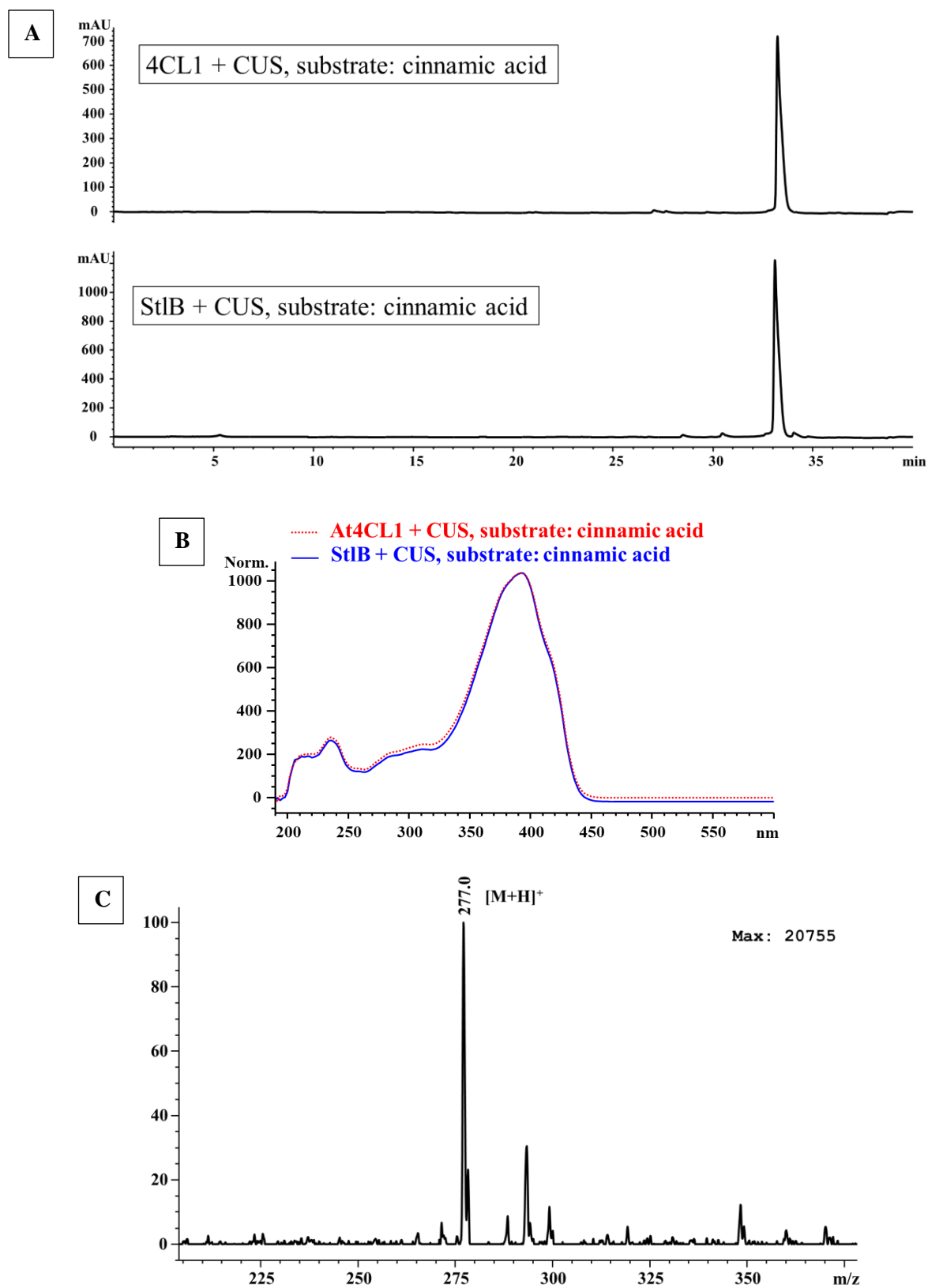


Figure A.4: Confirmation of dicinnanoylmethane formation by StlB with (A) retention time analysis, (B) UV-Vis spectral analysis and (C) ESI-MS spectral analysis